CZECH UNIVERSITY OF LIFE SCIENCES PRAGUE

Faculty of Forestry and Wood Sciences

Department of Genetics and Physiology of Forest Trees

Česká zemědělská univerzita v Praze

Fakulta lesnická a dřevařská

The drought effect on circadian dynamics of stem growth

MASTER'S THESIS

Prague 2022

Author: Bc. Jorge Palmero Barrachina

Supervisor: doc. Ing. Ivana Tomášková, Ph.D.

Declaration

"I hereby declare that I have done this thesis entitled "The drought effect on circadian dynamics of stem growth" independently, all texts in this thesis are original, and all the sources have been quoted and acknowledged by means of complete references and according to Citation rules of the FLD."

In Prague,

.....
Bc. Jorge Palmero Barrachina

CZECH UNIVERSITY OF LIFE SCIENCES PRAGUE

Faculty of Forestry and Wood Sciences

DIPLOMA THESIS ASSIGNMENT

Bc. Jorge Palmero Barrachina

Forestry Engineering
Forest Engineering

Thesis title

The drought effect on circadian dynamics of stem growth

Objectives of thesis

The goal of the thesis will be the description of stem circadian cycle in Norway spruce and the proportions of different phases during the years.

Methodology

The data from dendrometers (stem increment sensors DR 26, EMS Brno, CR) are being recorded from 2018 in Kostelec experimental sites (49,99N, 14,85E). The data are obtained in 10minutes intervals from April till October every year.

For the data analysis, the package “dendrometerR” in R studio will be used (van der Maaten, 2016). The package can handle various functions to import, verify, process, and plot high-resolution dendrometer using daily and stem-cycle approaches. The thesis established three goals:

a. Estimate the influence of prolonged drought and subsequent bark beetle attack and correlate them with different phases of circadian phases. The null hypothesis expects a lower number of days with stem radius increment (SRI) in trees affected by bark beetle compared to healthy one.

b. Estimate the effect of combined stress (drought x bark beetle attack) with respect to the weather of the studied year. SRI values will be extracted and correlated with meteorological data.

c. As the sap flow sensors (EMS81, EMS Brno, CR) are used simultaneously with the dendrometers the relationship between plant water status and stem radius variation will be evaluated.

The proposed extent of the thesis

50-60 pages

Keywords

dendrometer, diurnal cycle, drought, stem growth, transpiration

---

Recommended information sources

Balducci, L., Deslauriers, A., Rossi, S., & Giovannelli, A. (2019). Stem cycle analyses help decipher the nonlinear response of trees to concurrent warming and drought. Ann For Sci, 76(3), 1–18.

Deslauriers, A., Anfodillo, T., Rossi, S., & Carraro, V. (2007). Using simple causal modeling to understand how water and temperature affect daily stem radial variation in trees. Tree Physiol, 27(8), 1125–1136.

Deslauriers, A., Morin, H., Urbinati, C., & Carrer, M. (2003). Daily weather response of balsam fir (Abies balsamea (L.) Mill.) stem radius increment from dendrometer analysis in the boreal forests of Québec (Canada). Trees, 17(6), 477–484.

Fitter, A. H., & Hay, R. K. M. (2012). Environmental physiology of plants. Academic press.

Köcher, P., Horna, V., & Leuschner, C. (2012). Environmental control of daily stem growth patterns in five temperate broad-leaved tree species. Tree Physiol, 32(8), 1021–1032.

Larcher, W. (2003). Physiological plant ecology: ecophysiology and stress physiology of functional groups. Springer.

van der Maaten, E., van der Maaten-Theunissen, M., Smiljanić, M., Rossi, S., Simard, S., Wilmking, M., … Bouriaud, O. (2016). dendrometeR: Analyzing the pulse of trees in R. Dendrochronologia, 40, 12–16.

Vieira, J., Rossi, S., Campelo, F., Freitas, H., & Nabais, C. (2013). Seasonal and daily cycles of stem radial variation of Pinus pinaster in a drought-prone environment. Agric For Meteorol, 180, 173–181.

Expected date of thesis defence

2021/22 SS – FFWS

The Diploma Thesis Supervisor

doc. Ing. Ivana Tomášková, Ph.D.

Supervising department

Department of Genetics and Physiology of Forest Trees

Electronic approval: 15. 2. 2022

prof. Ing. Milan Lstibůrek, MSc., Ph.D.

Head of department

Electronic approval: 15. 2. 2022

prof. Ing. Róbert Marušák, PhD.

Dean

Prague on 08. 04. 2022

Acknowledgements

I am thankful to my supervisor Ivana Tomášková for offering me such an interesting issue to study and for helping me during these two years of work. I am also deeply thankful to Mehmet Özçelik for spending so much time looking for and preparing the best data. I would like to thank Emil Cienciala, who spent many hours with me visualising and making me understand the data. His advice was the guide which steered my steps to finally choose the correct humid and dry conditions for the thesis. I would like to thank Nela Gloriková, and other members of her team, for helping me with the statistical part of the attacked and healthy trees. Also, I want to thank Roman Modlinger for checking the part of the bark beetle and giving me support with my decisions to get the results.

ABSTRACT

Nowadays, Norway spruce (*Picea abies* (L.) Karst.) is the most threatened commercial tree species in Central Europe. The main reason for that is because of drought stress which is increasing both in frequency and intensity due to climate change. Automatic band dendrometers can evaluate tree water status and determine tree circadian phases. These two parameters are significantly correlated with growth and tree vitality. This study was focused on the description of circadian phases of Norway spruce during which years using data from 25 trees in Kostelec nad Černými Lesy, Czech Republic. Drought stress, bark beetle attack, and the combination between these two stress factors were evaluated. To calculate the distribution of circadian phases the package "dendrometeR" was used in the free software R studio. The drought stress was evaluated by comparing dry and control periods with the same day of the year. The effect of bark beetle attack was tested by using a generalised linear model with negative binomial distribution and likelihood-ratio test. Our description of the circadian phases showed that Norway spruce trees were physiologically active during the months of January to March. Months with less rainfall showed the smallest amount of Stem Radius Increment (SRI). The month of June showed the highest SRI values, being also the month with more precipitation. The duration of circadian cycles kept almost constant during these months. Contraction phase was significantly longer during the dry period. In terms of stem size variation, the expansion and SRI phases showed significantly lower values in the dry period. Healthy and attacked trees responded independently during the dry period. The evaluation of plant water status showed that trees were almost not transpiring during the dry period. Precipitation was the strongest meteorological variable that can influence the SRI. Sap flow was significantly correlated with contraction phase. We propose that bigger samples of bark beetle attacked trees with automatic dendrometers should be analysed after and before the attack.

Key words: Automatic band dendrometer, stem circadian cycle, stem radius increment, maximum daily shrinkage, drought, stand transpiration, bark beetle

ABSTRAKT

Smrk ztepilý (*Picea abies* (L.) Karst.) je současné době nejohroženější hospodářskou dřevinou střední Evropy. Hlavním důvodem je stres způsobený suchem, jehož četnost i intenzita se v důsledku klimatických změn zvyšuje. Pomocí automatických páskových dendrometrů je možné vyhodnotit stav vody ve stromě a určovat cirkadiánní fáze stromu. Tyto dva parametry významně korelují s růstem a vitalitou stromů. Tato studie byla zaměřena na popis cirkadiánních fází smrku ztepilého v průběhu několik let s využitím dat z 25 stromů v Kostelci nad Černými Lesy v České republice. Hodnocen byl stres suchem, napadení kůrovcem a kombinace těchto dvou stresových faktorů. K výpočtu rozložení cirkadiánních fází byl použit balíček "dendrometeR" ve volně dostupném softwaru R studio. Stres suchem byl hodnocen porovnáním suchého a kontrolního období ve stejný den v obou letech. Vliv napadení kůrovcem byl testován pomocí zobecněného lineárního modelu s negativním binomickým rozdělením a testu poměru věrohodností. Náš popis cirkadiánních fází ukázal, že smrky ztepilé byly fyziologicky aktivní od ledna až března. Měsíce s menším množstvím srážek vykazovaly nejmenší přírůstek poloměru kmene (SRI). Nejvyšší hodnoty SRI vykazoval měsíc červen, který byl zároveň měsícem s větším množstvím srážek. Délka cirkadiánních cyklů v jednotlivých měsících byla téměř konstantní. Fáze kontrakce byla výrazně delší během suchého období. Z hlediska variace průměru kmene v mikrometrech vykazovaly fáze expanze a SRI v suchém období výrazně nižší hodnoty. Zdravé a napadené stromy reagovaly během suchého období nezávisle. Hodnocení stavu vody v rostlinách ukázalo, že stromy v období sucha téměř netranspirovaly. Srážky byly nejsilnější meteorologickou proměnnou, která může ovlivnit SRI. Průtok mízy významně koreloval s fází kontrakce. Navrhujeme, aby bylo automatickými dendrometry analyzováno větší množství stromů před a po napadení kůrovcem.

Klíčová slova: Automatický pásový dendrometr, cirkadiánní cyklus kmene, přírůstek poloměru kmene, maximální denní smrštění, sucho, transpirace porostu, kůrovec

Contents

List of Tables

List of figures

List of the abbreviations used in the thesis

DBH	Diameter at breast height
DD	Degree days
DOY	Day of the year
GCC	Global climate change
GLM	Generalized linear model
GRO	Irreversible growth
MDS	Maximum daily shrinkage
PAR	Photosynthetic active radiation
SRI	Stem radius increment
SWP	Soil water potential
TWD	Tree water deficit
VPD	Vapor pressure deficit

1. Introduction

Impact of drought, heatwaves and extreme events caused by global climate change (GCC) are becoming more frequent and intense in the biosphere of our planet. and its environmental impact on tree growth is getting evident. GCC is changing the distribution of precipitations, causing impacts on seasonal water deficit, especially in Central Europe (Marek et al. 2011; Brázdil et al. 2009).

Automatic dendrometers can continuously record, in high frequency and accuracy, measurements of stem size, which are nowadays considered valuable information for analysing and predicting wood production, wood growth phenology, and tree water status (Drew, Downes 2009). Rhythmical variations in stem size are known as circadian rhythms, which can be analysed with two mathematical models: the stem daily approach and the cycle approach. The cycle approach is more used for dividing sub-diurnal stem size variation into mathematically defined phases and might be a tool for better understanding the effects of different factors on stem radial variations (Drew, Downes 2009; Deslauriers et al. 2011; van der Maaten et al. 2016).

Norway spruce is one of the most important tree species in Europe (San-Miguel-Ayanz et al. 2016). Its economic importance comes from its good timber qualities, suitable for construction and for paper production. The wood have excellent resonance properties for making instruments such as violins (Burckle, Grissino-Mayer 2003; Stoel, Borman 2008). This tree species has also been used to control soil erosion (Praciak et al. 2013).

Stress conditions such as droughts have a negative significant effect on tree metabolism by reducing photosynthesis and tree biomass (Tariq et al. 2018). Recent studies have proven that heatwaves have negative effects on tree water deficit (Salomón et al. 2022). Drought has been directly related to bark beetle attacks. In fact, it has been proved that the probability of bark beetle attack increases with drought stress conditions (Netherer et al. 2021; Matthews et al. 2018).

The principal aim of this study was the description of stem circadian cycle in Norway spruce and the proportions of its different phases during the time. Data from automatic band dendrometers was collected in periods of drought and normal conditions, and from healthy and attacked trees by the bark beetle. the thesis establishes three other goals: 1) Estimate the influence of prolonged drought and subsequent bark beetle attack; 2)

Estimate the effect of combined stress (drought x bark beetle attack); 3) the relationship between plant water status and stem radius variation will be evaluated

2. Literature review

2.1. The Norway Spruce (*Picea abies* (L.) Karst.)

Norway spruce (*Picea abies* (L.) Karst.) (Figure 1) is a large coniferous tree, which height can reach up to 50-60 m with a trunk diameter up to 150 cm. Normally, this tree species can reach an age between 200 and 300 years. The crown is usually conic, columnar, including whorled, short and stout branches. Buds are reddish brown, with a length around 5 mm with an acute apex. Needles are 1-2.5 cm long, 4-angled in cross section, rigid, light to dark green with fine white speckled lines. This tree species is monoecious, with unisexual flowers normally appearing when the tree reaches an age of 20-30 years (around 40 years in dense stands). Male flowers are located commonly at the base of the preceding year's shoot 1-2,5 cm long, globular, deep red in colour and then yellow when mature. Female flowers are located usually at the tip of the shoot, with dark red colour and 5 cm long, erect before pollination, becoming pendent afterwards. Cones are cylindrical, between 12 and 15 cm long, green before maturity, turning brown in autumn. When dry the cones open to disperse winged seeds, which are around 4 mm. The bark is orange brown colour. The wood is creamy white and simple to work (San-Miguel-Ayanz et al. 2016).

Figure 1: Picea abies *(L.) Karst. Source: https://herbaria.plants.ox.ac.uk/bol/Content/Projects/plants400/images/hires/PICEA_ABIES_LAMBERT_T25.JPG*

2.1.1. Distribution, habitat, and ecology

The Norway spruce is one of the most important trees in Europe, both economically and ecologically. Its native distribution (see Figure 2) is in boreal and subalpine coniferous forests, from the mountainous areas of central Europe to northern and eastern Europe. Its altitudinal range covers from 0 to 2400 metres above sea level. It is currently an introduced and naturalised species in various parts of Europe, such as the Pyrenees (San-Miguel-Ayanz et al. 2016). However, since the natural distribution of tree species depends on climate, landscape topography, and soil properties, the change in climatic parameters have the potential to affect their abundance (Hanewinkel et al. 2013).

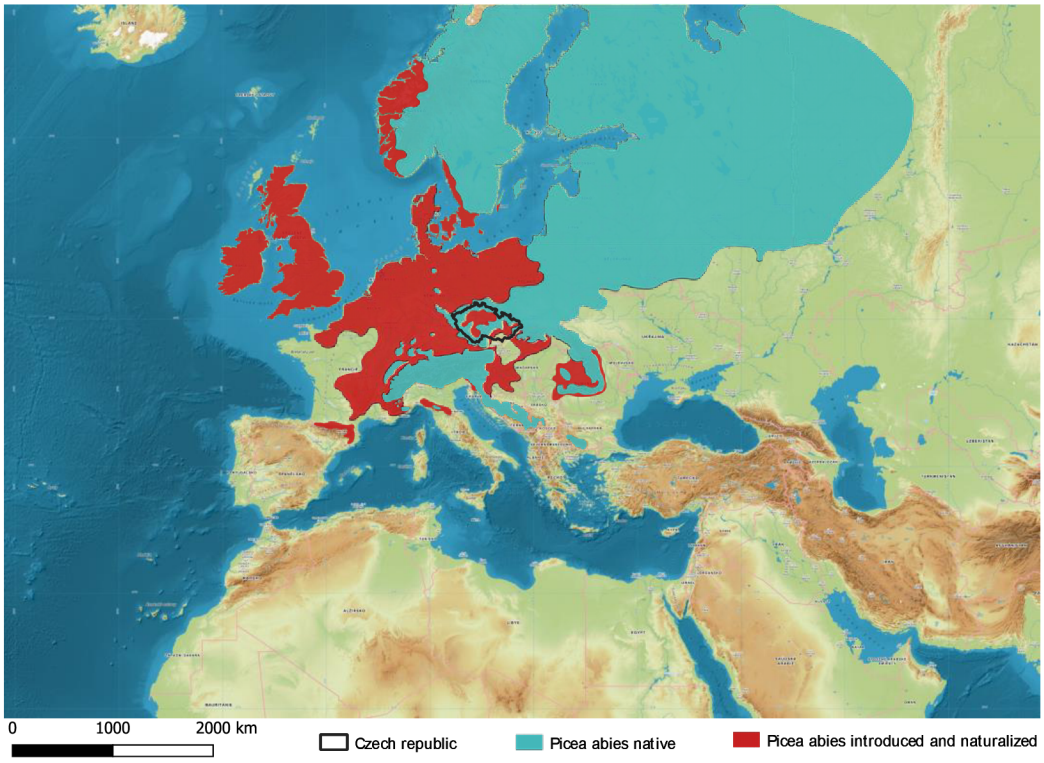

Figure 2: Distribution of Picea abies *(L.) Karst. The map was made with Qgis using the shape-files data of Caudullo et al., (2017).*

The Norway spruce tree has been also introduced in other countries outside Europe, such as the United States, Canada, Japan, South Africa, Tasmania and New Zealand (Svenning, Skov 2004; Taylor, Morin, Press 1993). This tree species is shade-tolerant, with rapid growth after 5 to 10 years of age. Norway spruce can grow in most substrates but prefers acidic soils. Also, Norway spruce trees have acidifying soils ability (Augusto et al. 2002; Holuša et al. 2018).

2.1.2. Importance and usage

Norway spruce is the most economically important tree species in the Czech Republic today and one of the most important in Europe. In year 2020, Norway spruce covered the 48.8% of the total forest area in the Czech Republic (*Zpráva o stavu lesa a lesního hospodářství 2020 (Lesy, eAGRI)*; San-Miguel-Ayanz et al. 2016). The economic importance of Norway spruce tree species comes from its good timber qualities. Norway spruce wood is a suitable building material, that has been used for construction of bridges, mining timbers, and ship masts. Also, this wood material is economically valuable for paper production. Its texture, weight, and bright uniform colour are greatly valued. The Norway spruce wood has low content of resin, which facilitates its use in the production of barrels, wooden boxes, and other packaging materials. The wood has excellent resonance properties for making instruments such as violins. However, the mechanical processing of this wood material is problematic due to the presence of frequent hard and dark-coloured knots (Burckle, Grissino-Mayer 2003; Stoel, Borman 2008; Surmiński 2007). In terms of its ecological importance, the Norway spruce has been used to control soil erosion. Moreover, its fast-growing capability, makes it a crucial tree species to store carbon from the atmosphere (Praciak et al. 2013; Marek et al. 2011).

2.1.3. Threats and diseases

Droughts, fires, storms and pathogens such as *Heterobasidian annosum*, *Armillaria* and bark beetle (*Ips typographus*) are the most important disturbance factors for Norway spruce tree species. Holuša et al. (2018) noted that the ability of Norway spruce to acidify soils makes it more susceptible to be attacked by armillaria, due to the fact that this pathogen proliferates faster in acidic conditions. *Ips typographus* (L.) is the major pest in European forests. This bark beetle can cause extensive damage to Norway spruce stands by feeding in the phloem and by inoculating pathogenic blue stain fungi (Sallé et al. 2003). In the Czech Republic, the attacks of bark beetle are devastating the Norway spruces forests, both in its native and naturalized area. The volume of Norway spruce wood attacked by the bark beetle has been increasing last year (see Figure 3), reaching huge amounts of wood such as 20,703 and 21,904 thousands of m^3 in years 2019 and 2020 respectively. Furthermore, drought has been directly related with bark beetle attacks. As a matter of fact, it has been proved that probability of bark beetle attack increases when trees are in drought stress conditions (Netherer et al. 2021; Matthews et

al. 2018). However, effects of drought on bark beetle-induced Norway spruce mortality are still poorly understood (Netherer et al. 2021).

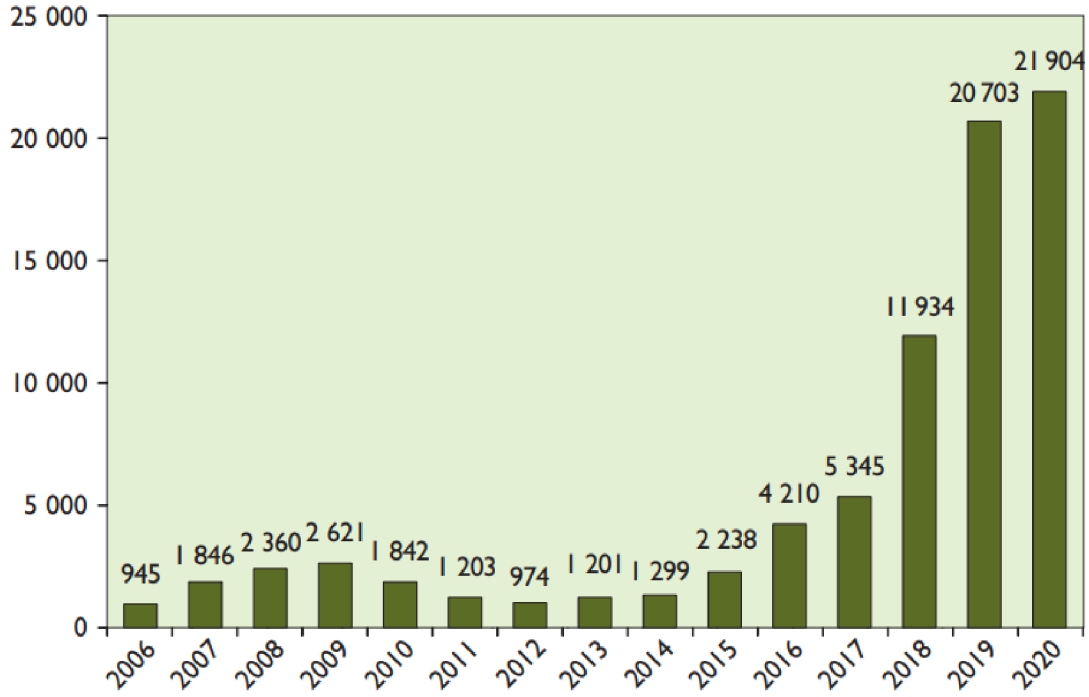

Figure 3: Recorded harvested Norway spruce wood volume attacked by bark beetle in the period 2006-2020 (thous. m³) Source:(Zpráva o stavu lesa a lesního hospodářství 2020 (Lesy, eAGRI) *2021)*

2.2. Bark beetle

Ips typographus (Figure 4), family *Curculionidae* and order *Coleoptera*, is a moderate to large (4.2-5.5 mm), cylindrical, brown bark beetle with an excavated elytral declivity, which includes laterally 4 spines on each side from above, erect yellow hairs are sticked out from the body perimeter and margins of the declivity (Cavey, Passoa, Kucera 1994). The head is not visible when viewed dorsally and it is concealed by a thoracic shield. (*Ips typographus (L.), European Spruce Bark Beetle Screening Aid*)[1].

[1] https://www.barkbeetles.org/exotic/htypgrph.html

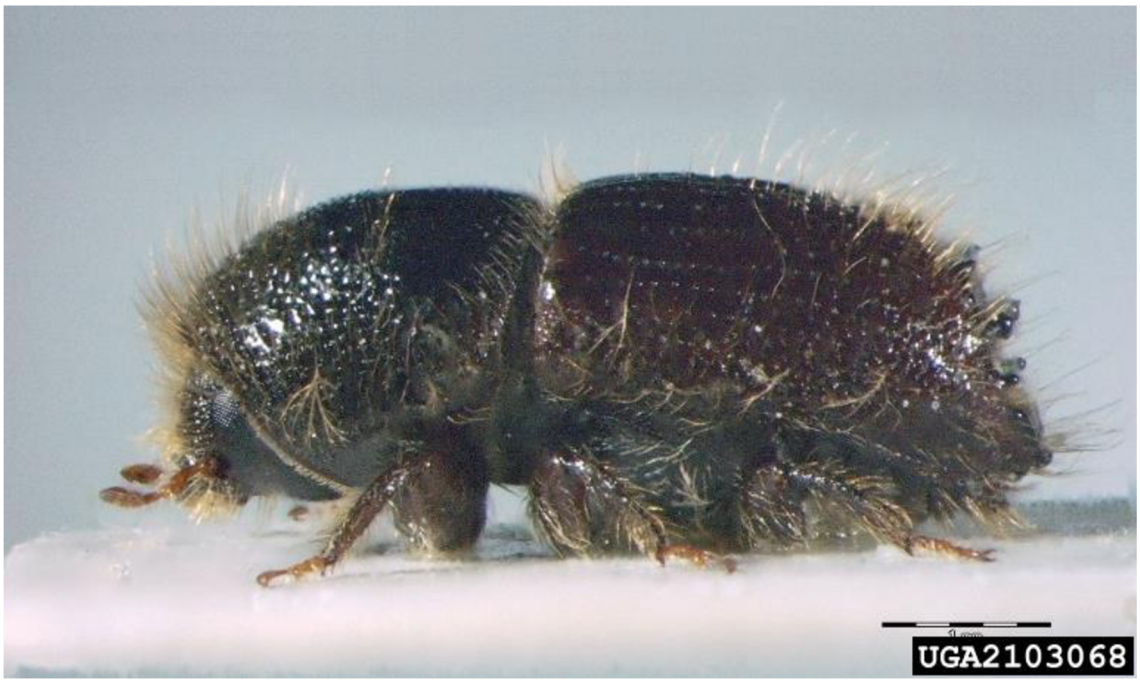

Figure 4: Ips typographus. *Source:* <*https://www.invasive.org/browse/subinfo.cfm?sub=888*>

"Bark beetle" is both a taxonomic and ecological designation. In the taxonomic sense, bark beetles are all species in the weevil subfamily *Scolytinae*, counting also species that do not consume bark. However, in the ecological sense, bark beetles are species of *Scolytinae* whose larvae and adults live and feed in the phloem of trees and other woody plants (Hulcr et al. 2015, p. 2).

Baier, Pennerstorfer, Schopf (2007) made an algoritmus called PHENIPS – "A comprehensive phenology model of *Ips typographus*" which was based on the concept of degree-days (DD). The use of DD for calculating the temperature dependent development is widely accepted as a basis for building phenology and population dynamics models (Roltsch et al. 1999). Wermelinger and Seifert (1998) noted that the lower limit in temperature for *Ips typograhus* is 8.3°C and the upper limit 38.9°C.

Flight activity starts after the amount of air temperatures (AT) are above of 16.5°C and when $\sum(ATmax - 8.3) \geq 140DD$ (Baier, Pennerstorfer, Schopf 2007; Lobinger 1994) ≈ from 1 April in the Czech Republic. Development of each stage depends on the average temperature of the phloem. Development is finished when $\sum(ATmax - 8.3) = 557$ DD. Re-emergence of parental beetles occurred at a time when 49.7% of the thermal sum for total development (557 DD).

In winter, the shortening day length and low night temperatures in late summer are two major parameters that induce diapause, physiological state in which adult leafcutters hibernate. During diapause, individuals do not take food or only in very small amounts (Hahn, Denlinger 2007). Flying muscles and fat body development are reduced. Diapause is completed around mid-December (after frost). Shortening the day also influences the end of reproduction, which terminates after shortening the day to about 15 hours, i.e. approximately mid-August (McManus, Liebhold 2003).

2.3. Drought, Heatwaves and Climate change

Extreme climatic events as heatwaves and droughts are expected to become more frequent in a global warming (Rahmstorf, Coumou 2011). The heatwaves, which are generally defined as periods of consecutive days with anomalously high temperatures, have been increasing during the last decades and are expected to keep increasing (Barriopedro et al. 2011). Heatwaves are often accompanied by anomalies in other meteorological parameters such as a lack of rainfall and high evaporative demand. (Zscheischler et al. 2018). Thus, drought stress intensifies the negative effects of extreme temperatures on tree productivity, vigour and survival (Teskey et al. 2015; Tariq et al. 2018). Temperate forests are expected to be specifically vulnerable to drought and soil drying due to the fact that they are not adapted to such conditions (Salomón et al. 2022).

To understand the effect of drought on tree productivity, it is important to clarify what is drought. There are, numerous definitions of drought which can be grouped in four categories (Mishra, Singh 2010):

i. **meteorological drought**, which is the lack of precipitation over a region for a period of time
ii. **hydrological drought**, which is related to a period with not enough surface and subsurface water resources for established water uses of a given water resources management system.
iii. **agricultural drought**, refers to a period with decreasing soil moisture and consequent crop failure.
iv. **socio-economic drought** associated with failure of water resources systems to meet water demands and in this way associating droughts with supply of and demand for an economic good (water).

In this thesis, we will refer to drought as the third definition of drought because in terms of tree productivity it is crucial to consider the factor soil moisture. Thus, drought is not only lack of precipitation, but the lack of available water in soil.

2.3.1. Soil water balance, field capacity and wilting point

Soil is a heterogeneous multiphase porous system, which contains three natural components: (1) the solid phase (mineral particles and solid organic materials); (2) the liquid phase (or soil solution); and (3) the gaseous phase (Rai, Singh, Upadhyay 2017). The soil acts as a reservoir of water with a maximum storage capacity, related to the saturation moisture. There is also a maximum soil water storage held against gravity, which is known as field capacity, and a minimum water content below which plants cannot extract water (Lidón, Ramos, Rodrigo 1999).

Field capacity depends on numerous factors, as (i) previous soil water history, (ii) soil texture and structure, (iii) type of clay, (iv) organic matter, (v) temperature influence, (vi) water table, (vii) depth of wetting field capacity, (viii) presence of impeding layers (e.g., clay, sand, gravel) and (ix) evapotranspiration[2] (Kirkham 2005).

The minimum water content is also known as the permanent wilting point, which depends on plant variety, but it is usually around -1,500 kPa (-15 bars) (Rai, Singh, Upadhyay 2017). Permanent wilting point is broadly used to ascertain plant resistance against drought stress (Garg et al. 2020).

With field capacity (FC) and the permanent wilting point (WP), available water (AW) can be calculated (equation 1)

$$AW = FC - WP \quad (1)$$

2.3.2. Soil water potential as indicator of the wilting point

Both field capacity and the permanent wilting point are precise values that can be measured by studying the soil, however, if one cannot measure field capacity in the field, it is often estimated to be the soil water content at a soil matric potential of −0.03 MPa (-1/3 bar). The permanent wilting point, it is usually estimated to be the water content at a soil matric potential of −1.5 MPa (−15 bars). The permanent wilting point depends upon plant osmotic adjustment. Some plants can absorb water from soil at potentials much

[2] The rate and pattern of extraction of water by plant roots from soil

lower than this (−6.0 MPa ≈ -60 bars) (Kirkham 2005). In this thesis, we considered a dry period when the soil water potential was lower or equal to -15 bars.

2.3.3. Sap flow as indicator of dry periods in forests

Sap flow means flow of water from roots to leaves. The principal method to measure sap flow is the heat balance. Steel plate electrodes are inserted into the stem of the trees and are heated by flow of electric. It is possible to maintain the temperature of the sensor constant by changing the power input (voltage). Part of the heating energy is dissipated into the surroundings by heat conductivity of the xylem tissue while the rest is carried away by sap flow. In other words, when water is running from roots to leaves, water flux cools the electrodes, thus more power input is needed to keep the temperature of electrodes constant. The heat balance calculates the water flux (or the amount of water in terms of mass or volume) by using the power input and temperature rise of water passing through the heated space. For more details, we present the equations from the web-site EMS Brno[3] (Equation 2).

$$P = Q \times dT \times c_w + dT \times z \quad (2)$$

Where:

- P is power of heat input [W]
- Q is sap flow rate [kg s-1]
- dT is temperature difference within the measuring point
- c_w is specific heat of water [J $kg^{-1}K^{-1}$]
- z is coefficient of heat losses from the measuring point [W K-1].

Using equation 2, sap flow can be calculated as (Equation 3):

$$Q = \frac{P}{c_w \times d \times dT} - \frac{z}{c_w} \quad (3)$$

Where d is effective width of measuring point (5.5 cm). First term of this equation quantifies heat that is conducted by sap flow. Second term represents heat losses from the sensor, which can be estimated when sap flow approaches zero. In these equations, it is assumed that sap flow is equal to zero during the heavy rains or at night before sunrise.

Sap flow methods hold important advantages over other techniques for measuring of transpiration by individual branches, tillers, or whole plants. Sap flow methods are simply automated, so continuous records of plant water use with high time resolution can be obtained (Smith, Allen 1996). Many publications about tree physiology and response of

[3] http://www.emsbrno.cz/p.axd/en/Sap.Flow.large.trees.html

tree transpiration to drought used sap flow measurements (Brinkmann et al. 2016; Cienciala et al. 1998; Smith, Allen 1996; Stöhr, Lösch 2004). Tree transpiration can be obtained by dividing the total tree sap flow into its cross-sectional area at 1.3 m height. Tree transpiration can be upscaled to stand transpiration by using the basal area of the stand. Potential evapotranspiration can be calculated from meteorological variables and sap flow using the Penman-Monteith equations (Zotarelli et al. 2015).

Cienciala et al. (1998) observed the fact that under good weather conditions (sunny days with no clouds) and available water in soil, transpiration and sap flow measurements showed a curve which fitted with the potential evapotranspiration (figure 3, pine and spruce 1995). When sap flow curve was drawn in dry periods, its values started to continuously decrease day after day, and the difference between stand transpiration and potential evapotranspiration increased (Figure 3, pine and spruce 1994).

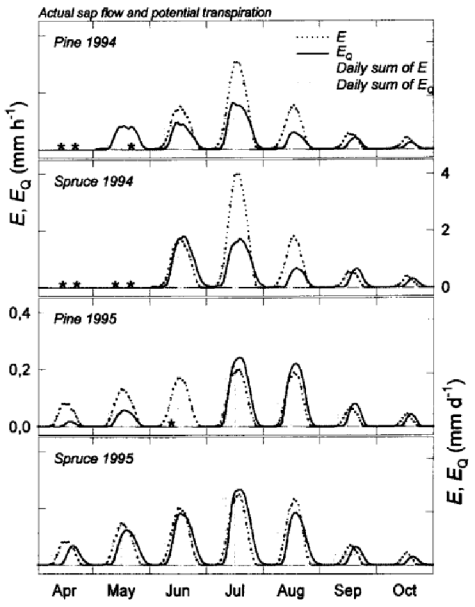

Figure 5: Water flux in boreal forest during two hydrologically contrasting years. Where E_Q *is the stand transpiration and* E *is the potential evapotranspiration. Source: (Cienciala et al. 1998)*

Van Camp et al. (2018) noted the fact that under good weather conditions and available water in soil, sap flow measurements had a bell-shaped curve (Figure 6, plots “e”, “f”, “g” and “h”). When there were dry conditions, the shape of the sap flow curve changed on hourly scale (Figure 6, plots “a”, “b”, “c” and “d”).

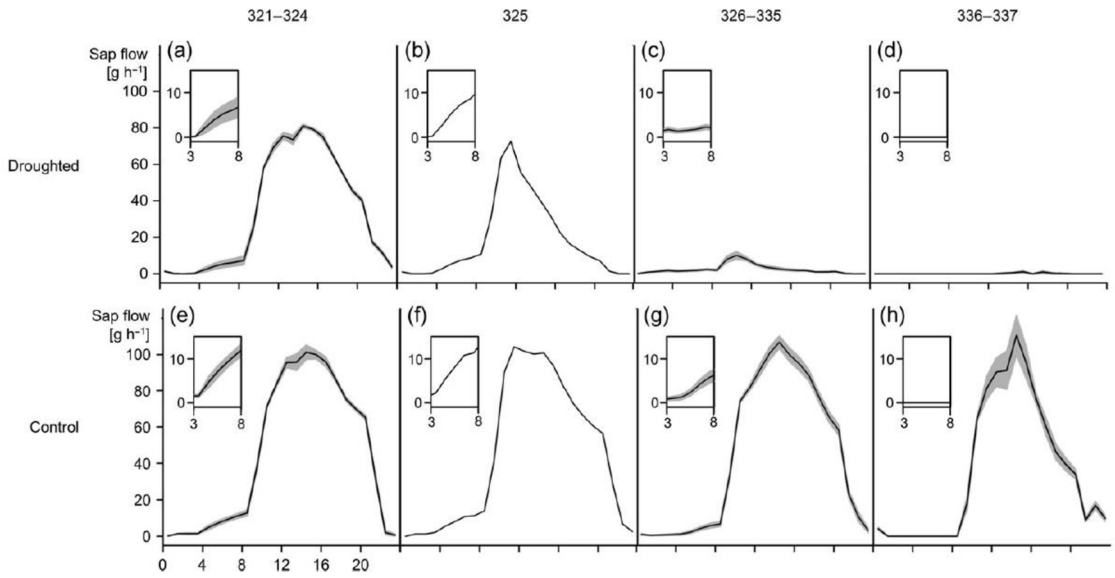

Figure 6: Hourly sap flow values drawn in dry and control periods. a), b), c) and d) show how sap Flow responds to dry periods. Pictures e), f), g) and h) how it responds to control periods. Source: (Van Camp et al. 2018)

Declining sap flow rates can be interpretated as a reduction of the tree's stomatal conductance. The purpose of reducing stomatal conductance is to conserve water and to avoid critically low water potentials that would put a tree at risk of hydraulic failure (Brinkmann et al. 2016).

2.4. Automatic Band Dendrometers

A dendrometer is an instrument normally used for measuring the diameter of the stems of trees. Two broad categories can be defined: those that contact the stem and those that do not. Band dendrometers, are those which are in contact with the bark of the stem and measure its circumference. This type of dendrometers have been broadly used in forest research and have been designed to measure at a wide range of resolutions. Nowadays, there are some dendrometers that have high spatial and temporal precision, which are collecting data that is becoming better recognized to commercial forestry (Drew, Downes 2009). These devices have been used to understand growth responses to climate and silviculture (Vieira et al. 2013; Belien et al. 2014; van der Maaten 2013). Deslauriers et al. (2003) used high-precision data, to assess the stem water status, proving that the variation of the balsam fir (*Abies balsamea* (L.) Mill.) diameter is significantly correlated with precipitation and high vapour pressure deficit. Other studies were analysing sub-diurnal stem size variation to determine the stem circadian cycle phases mathematically. Deslauriers et al. (2011) used a mathematical model in a SAS routine to determine the circadian phases, also known as circadian rhythms, from automatic dendrometer's data

using time series analysis. No such routine was available for the open-source statistical software R until 2016, when the package “dendrometeR” was created by van der Maaten et al. (2016). Two approaches can be calculated with this package: 1) the daily approach and 2) the cycle approach. Both approaches are explained in the next chapter.

2.4.1. The Stem Circadian Cycle

Rhythmical variations in stem size are known as circadian rhythms. Two mathematical models can describe these variations using high-temporal and spatial precision dendrometers. 1) The stem daily approach and 2) The stem cycle approach (Drew, Downes 2009).

The daily approach separates the data collected by the automatic dendrometers into 24 h intervals and determines the maximum, average and minimum value, and the time of day at which they occurred. Two variables can be calculated with this approach: the amplitude and the growth rate. Amplitude can be calculated as the difference between the maximum and minimum value of each day. The growth rate, or stem size variation, (ΔR) is usually quantified as the average (or maximum) diameter measurement of day "i+1" minus the measurement of the previous day "i" (Deslauriers, Rossi, Anfodillo 2007). Thus, positive and negative results can be obtained. Negative results will appear when the maximum diameter of the day “i+1” is lower the maximum diameter of day “i”. Otherwise, positive values will be obtained. As it has been seen in most temperate forests examined by dendrochronological analysis, summer rainfall is the prominent factor (if not the most important) which explains variation in ΔR. Soil moisture, temperature, and forest management activities have been found to be influential in many stands as well (Köcher et al., 2012).

The cycle approach is more used for dividing sub-diurnal stem size variation into mathematically defined phases and it might be a tool for better understanding the effects of different factors on stem radial variations. It has been proved that the radius of tree stems reaches a minimum in the mid-to late-afternoon and a maximum in the early morning, driven by water movement in the tree through the soil–plant–atmosphere continuum. This patterns of shrinkage during the day (especially with good weather conditions when the trees have open stomas and transpiration is happening) and expansion during darkly nights or heavy raining (with closed stomas and there is no transpiration) have been described in terms of five phases or three phases. In this thesis,

we used the three phases approach, which is summarised as follows (Drew, Downes 2009; Deslauriers et al. 2011; van der Maaten et al. 2016):

- Contraction (phase 1) – It is the period from a previous local maximum to a local minimum
- Expansion (phase 2) – It is the growth from a local minimum until the magnitude of the previous maximum
- Stem radius increase (phase 3) – It is the growth from a previous maximum to a new maximum.

Using the package dendrometeR, these phases can be determined and studied (see Figure 7). The package is capable to determine the beginning and the end of each phase and calculate its minimum and maximum values. The difference between maximum and minimum values of each phase is called “magnitude”. Magnitude is usually expressed in units of micrometres [µm]. The time that elapses between the maximum and minimum values of each phase is called "duration". Duration is usually expressed in units of hours [h]. It is important to say that some authors refer to phases 1 and 2 as “shrinkage” and “recovery” respectively. Both phases are usually studied for understanding the stem rehydration (Deslauriers et al. 2003).

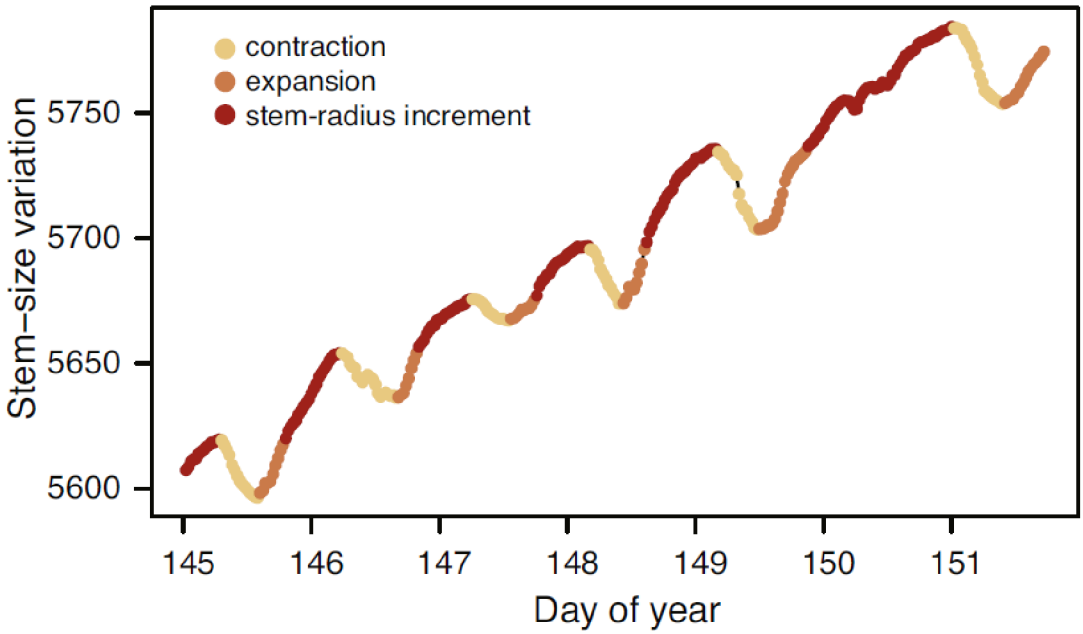

Figure 7: example of circadian phases plotted by the package dendrometeR. Source: (van der Maaten et al. 2016).

The stem circadian cycle usually lasts around 24 h, but due to meteorological variables as heavy rain in summer or freeze–thaw events in other seasons of the year might produce

long cycles of more than 24 h. cycles lasting around 24 h (± 3 h) are defined as regular (REG), those lasting more than 28 h were defined as long cycles (LG). The very short cycles are defined as those which lasts less than 20 h. However, this very short cycles are not very frequent compared with the long cycles and are used to be considered as regular (Deslauriers, Rossi, Anfodillo 2007).

2.4.2. Growth and Tree Water Deficit

Tree growth is a product of the interaction of genes and environment. However, this interaction is not the same for every species and individuals. Since the process of photosynthesis and maintenance of living trees requires some energy, the process of photosynthesis does not mean tree growth. In other words, some part of the photosynthesis is used to conserve the cells and different activities which do not imply growth. The part of the photosynthesis which is used for growing corresponds to the net primary production (NPP), while the gross primary production (GPP) is a synonym of all the energy produced by photosynthesis. The difference between the GPP and NPP is known as autotrophic respiration (Ra).

Time series of automatic dendrometers showed the fact that stem radius changes during time. During the day, when transpiration is high, the stem loses water from elastic tissues. This loss of water is proportional to a decrease in stem radius. This process is called tree water deficit (TWD). (Zweifel et al. 2016) stablished two concepts to quantify the growth and the tree water status from automatic dendrometer data: The LG concept (linear growth during periods of stem shrinkage) and the ZG concept (zero growth during periods of stem shrinkage).

The LG concept assumes a constant and positive growth rate between two peaks in stem radius data with the assumption that increasing tree water deficit (TWD) does not affect growth processes. This method can be used to compare peaks in stem radius data (Zweifel et al. 2016).

The ZG concept assumes no growth during periods of stem shrinkage (i.e. increased TWD). The result of this concept is a curve, which represents the irreversible stem expansion (GRO), with a stepwise shape.

Mathematically, TWD and GRO can be formulated as:

$$GRO_{(t)} = \begin{cases} SR(t) - \max\,[SR(< t)], & SR(t) \geq \max\,[SR(< t)] \\ 0, & SR(t) < \max\,[SR(< t)] \end{cases} \quad (4)$$

$$TWD_{(t)} = \begin{cases} \max[SR(< t)] - SR(t), & SR(t) < \max\,[SR(< t)] \\ 0, & SR(t) \geq \max\,[SR(< t)] \end{cases} \quad (5)$$

Where GRO is irreversible stem expansion, SR is stem radius data and TWD is tree water deficit. t refers to the current record, < t refers to historical records. For a better understanding, Figure 8 shows the calculations of GRO and TWD.

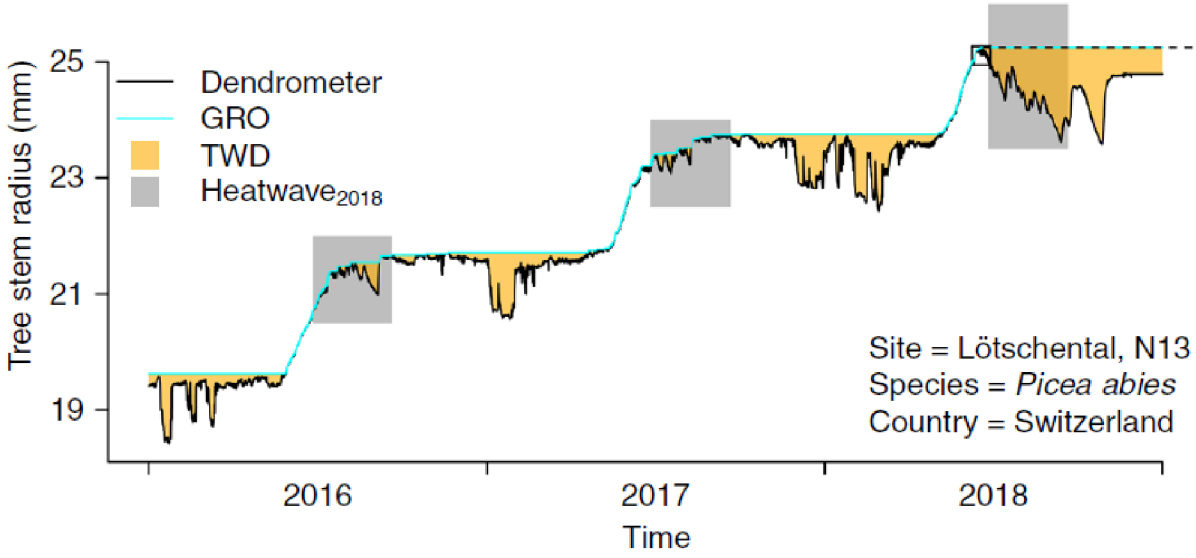

Figure 8: Example of irreversible growth (GRO) and tree water deficit (TWD) calculated from automatic dendrometer data. Source: (Salomón et al. 2022)

Salomón et al. (2022) used the concept zero-growth to analyse high-resolution dendrometers (see Figure 8). To quantify how much the drought can influence the net growth and rehydration of many broadleaf and conifer species used a sample of 157 trees in 37 different locations around Europe during three different years. Year 2018, with extremely hot and dry conditions and other years (2016 and 2017) as control years. Relative to the two control years, GRO was not significantly reduced by the hot and dry year, but stems experienced twice the temporary shrinkage (or contraction) due to depletion of water reserves. The Norway spruce, showed particularly less capability of rehydrating overnight than broadleaves across gradients of soil and atmospheric drought, suggesting less resilience toward transient stress.

3. Aims of the Thesis

The principal goal of the thesis will be the description of stem circadian cycle in Norway spruce and the proportions of different phases during the years.

As data was collected in dry and normal conditions periods, and from healthy and attacked trees by bark beetle, the thesis establishes three more goals:

1. Estimate the influence of prolonged drought and subsequent bark beetle attack and correlate them with different phases of circadian phases. The null hypothesis expects a lower number of days with stem radius increment (SRI) in trees affected by bark beetle compared to healthy one
2. Estimate the effect of combined stress (drought x bark beetle attack) with respect to the weather of the studied year. SRI values will be extracted and correlated with meteorological data
3. As the sap flow sensors (EMS81, EMS Brno, CR) are used simultaneously with the dendrometers the relationship between plant water status and stem radius variation will be evaluated

Based on the objectives we have set following hypothesis:

- H1: The dry period will limit the duration and magnitude of SRI in healthy trees
- H2: There should be a difference between the duration of SRI of the trees attacked by the bark beetle and the control trees during the dry period
- H3: There should be a difference between the duration of SRI of the trees attacked by the bark beetle and control trees before and after the attack

4. Methods

4.1. Site description

The study site was carried out in a forest near Kostelec-Praha (09' 48" - 41° 10' 55" N, 28° 57' 27" -28° 59' 27" E, see Fig. 9). Two localities, called site 3 and 4, were located under semi-humid climate conditions. The average annual temperature is 7.6°C, average annual precipitation is 665 mm and Lang's rain factor is 87.6 (according to the Meteorological Station of Czech Hydrometeorological Institute in Ondřejov, the average values for the period 1961–2000). The experimental plots are situated at the altitude of 430 m above sea level. The mineral bedrock is granodiorite (so-called Říčanská žula) covered by Luvisol, in some parts with transition to Pseudogley. Soils have good nutrition levels. Both sites are situated at plain or slight slope and the dominant tree species is Norway spruce.

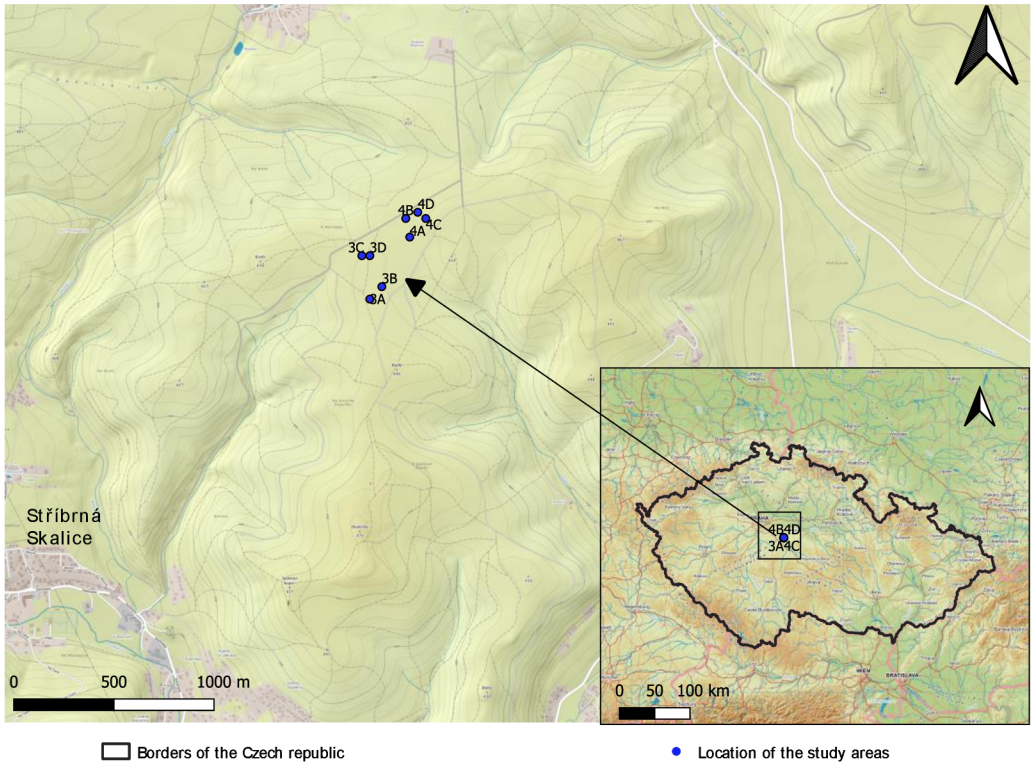

Figure 9: Location of the study site. Map made with Qgis. Coordinates in table 1.

Each plot was divided in four sub plots. Each sub plot was named with alphabetic letters from A to D.

Table 1: Coordinates of the study area.

Site	Longitude	Latitude
3A	14° 52' 26''	49° 54' 39''
3B	14° 52' 29''	49° 54' 41''
3C	14° 52' 24''	49° 54' 46''
3D	14° 52' 26''	49° 54' 46''
4A	14° 52' 36''	49° 54' 49''
4B	14° 52' 35''	49° 54' 52''
4C	14° 52' 40''	49° 54' 52''
4D	14° 52' 38''	49° 54' 53''

4.2. Data collection

Meteorological variables

Data for air temperature (Tair, [°C]) air relative humidity (RH, [%]), precipitation [mm] and photosynthetic active radiation (PAR, [µmol/m^2/s]) were collected with an automatic weather station during the study period. The weather station (EMS Brno, Czech Republic) was located at 2 m height in a bare open space close to the studied sites (<200 m in linear distance). Data were recorded with 5 minutes intervals and mean hourly values were calculated as an average of all measurements. The air vapor pressure deficit (VPD) was calculated by combining the air temperature and relative humidity according to the equation 6 (Campbell, Norman 1998):

$$VPD = 0.611 \times e^{[17.502 \times T/(240.97+T))] \times (\times 1 - HR)} \quad (6)$$

where VPD is air vapor pressure deficit (kPa), T is air temperature (°C) and RH is the air relative humidity (%).

Soil water potential (SWP) (Ψ, kPa) was recorded at topsoil (10 cm depth) with 5 soil water potential sensors in each sub plot with 10-minute intervals (Delmhorst Inc, New Jersey, U.S.A) and Microlog SP3 data logger (EMS Brno, Brno, Czech Republic) for each site. Mean daily SWP was calculated by averaging overall measurements from five sensors for each site.

Sap flow

Sap flow sensors (EMS 81, EMS Brno, Brno, Czech Republic) functioning according to the trunk heat balance method (equation 3, described in the chapter 2, Literature Review) were set on different trees in each site since 2018. Trunk heat balance method includes three heated electrodes and one reference (non-hetated, central) electrode placed 10 cm

below the upper electrodes. Tree trunks were covered with reflective shield after installation of the sensors to isolate the created field of temperature around the sensors from convective heat loss and effects of the sun (see Figure 10). A sample of 21 sensors were selected for the site 3 (6 sensors in sub plot A, 6 in sub plot B, 5 in sub plot C, and 4 in sub plot D). A sample of 4 sensors was selected in site 4 sub plot C.

Automatic band dendrometers

Automatic band dendrometers (sensor DRL26C, Brno, Czech republic) were installed in same trees as were sap flow sensors (see Figure 10). Data was collected in 10 minutes interval and mean hourly values were calculated as an average of all measurements.

Figure 10: Example of sensors. Sap flow meter EMS81 with isolation and automatic band dendrometer EMS81 without isolation.

4.3. The selected trees and periods for the study

In order to select the dry and normal periods for the study, first we looked into the soil water potential data. All periods which showed soil water potential lower than -15 bars were considered as dry periods. Two small dry periods were detected in year 2018 for site 4, from June 25th to 27th (DOY 176-178) and from October 22nd to 24th (DOY 295-297). The longest and driest period in year 2018 was recorded from August 13th to September 1st in site 4 (DOY 225-244), which shared the dry period with site 3 from August 19th to September 1st (DOY 231-244). Year 2019 was a normal year without dry periods. Despite there are some gaps in soil water potential of year 2019, precipitation and vapor pressure deficit do not show any signal of possible drought in this year. Year 2020 was dry in site 3 from September 21st to 24th (DOY 264-267). Data from soil water potential in site 4 was missing in this period (see Figure 11).

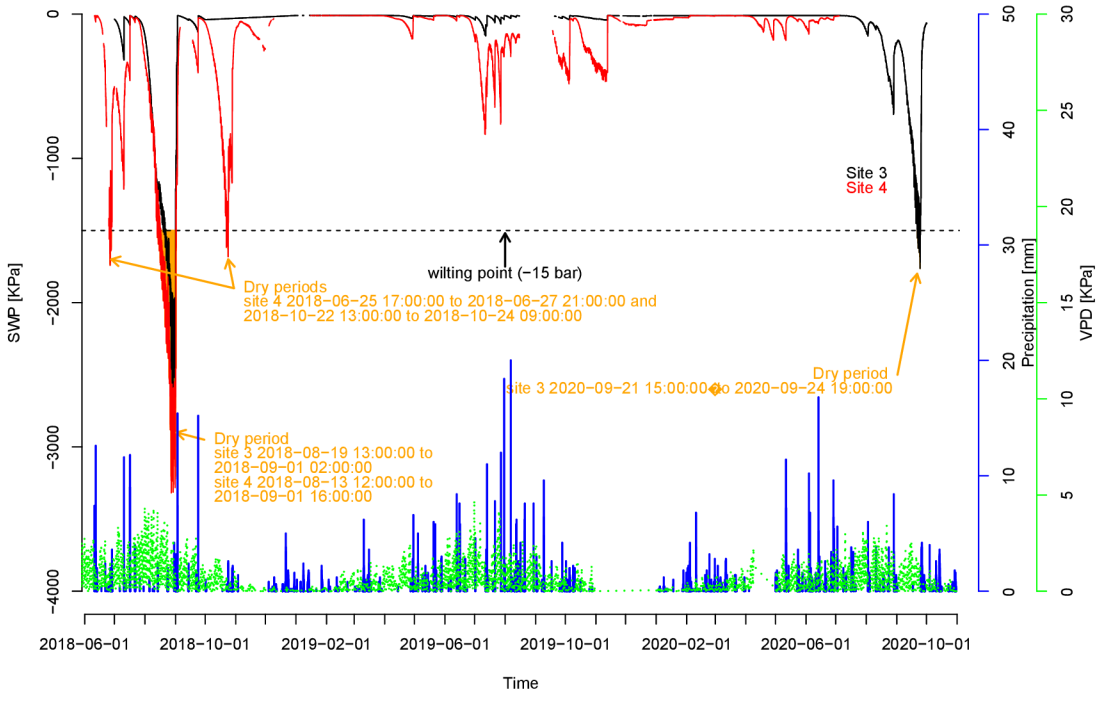

Figure 11: Dry and normal conditions for years 2018, 2019 and 2020. SWP [KPa] is soil water potential. Black and red lines correspond to site 3 and 4 respectively. VPD [KPa] is vapor pressure deficit (green dotted line). Precipitation [mm] is plotted with blue bars.

A sample of 21 trees in site 3 and 4 trees in site 4 was studied in this thesis. All trees in site 3 are in healthy conditions. Since year 2020 showed humid conditions and normal range of temperatures and there were less gaps in data than in other periods, we selected this year as the best candidate for studying the distribution of different circadian phases.

For studying the differences in circadian phases between dry and normal conditions, we decided to select the dry period from year 2018 DOY 225 to 244. The same DOY was selected in 2020 as a control period. Year 2019 could be also a control year, but because of the gaps shown in Figure 12, we decided to not consider this year for the study. All trees from site 3 were studied and compared between these two periods. Also, we did some supplementary calculations to compare the irreversible growth (GRO) and tree water deficit (TWD) between these two periods.

For comparing the attacked and healthy trees, we studied trees located in site 4 (see Figure 12) in three different periods: i) in dry conditions (DOY 225-244, year 2018); ii) one month before the attack (DOY 117-147, Year 2020); and iii) one month after the attack (DOY 150-185, Year 2020).

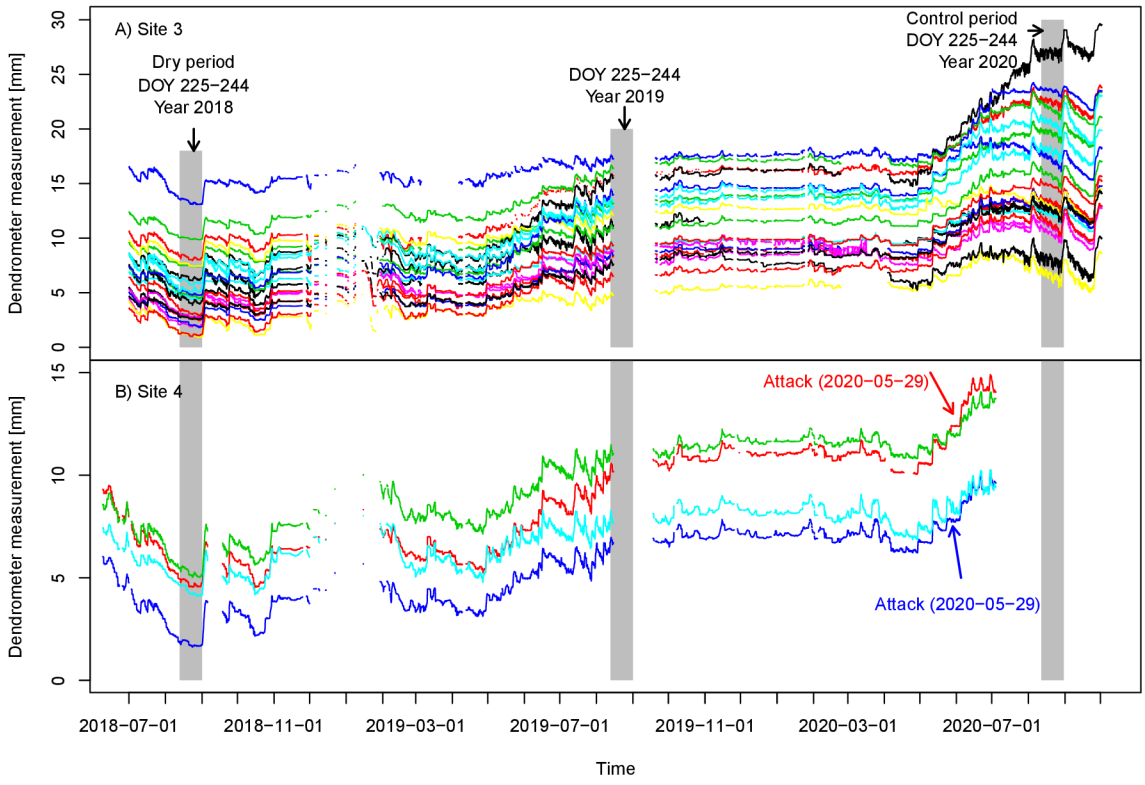

Figure 12: Trees and periods selected for the Thesis. Plot A) and B) shows single tree-dendrometer measurements (each line is a different tree) for site 3 and 4 respectively. Grey background are the same day of the year (DOY) in different years. The period from 225 to 244 covers the longest dry period detected in 2018. The same DOY are marked in control years (2019 and 2020). Red and blue arrows indicates the trees and the moment when the bark beetle attack was detected. Missing values are gaps due to lack of battery.

Table 2: Dimensions of the trees selected for the study. Codes with number 3 and 4 correspond to site 3 and 4 respectively. Characters A, B, C and D correspond with different sub-plots of each site.

Code	N	DBH [cm]	Bark [mm]	Circumference [cm]	
3A2	1	40	--	--	
3A4	2	38	7	106	
3A5	3	36	7	103	
3A6	4	30	7	86	
3A8	5	33	5	96	
3A10	6	41	7	110	
3B2	7	41	9	122	
3B3	8	37	7	100	
3B5	9	43	8	134	
3B6	10	35	6	106	
3B9	11	38	8	108	
3B10	12	47	8	139	
3C2	13	37	7	103	
3C5	14	36	8	105	
3C7	15	38	9	112	
3C8	16	35	6	105	
3C10	17	31	6	97	
3D3	18	34	7	103	
3D4	19	36	8	104	
3D6	20	40	6	121	
3D8	21	43	9	122	
4C3	22	54	9	145	*
4C5	23	43	8	124	
4C8	24	33	6	97	*
4C1	25	40	7	116	

N – Tree nº; DBH – diameter at breast height; (*) Attacked trees by the bark beetle

4.4. Data processing

4.4.1. Dendrometer data

Four parameters were derived from automatic band dendrometer data; 1) Growth rate; 2) Irreversible growth (GRO); iii) Tree Water Deficit (TWD); and iv) The Stem Circadian Phases.

Growth rate calculation

Growth rate, or stem size variation, was calculated as the difference between the daily mean values of stem diameter of two consecutive days (Deslauriers, Rossi, Anfodillo 2007). These mean values were obtained using the daily approach from the R package dendrometeR (van der Maaten et al. 2016).

Irreversible growth (GRO) and Tree Water Deficit (TWD)

For a better comparison with Salomón et al. (2022), we calculated GRO and TWD for the same day of the year as they used (DOY 208-264). Dry period was in year 2018 and control period in 2020. We used equations 2 and 3 (written in the literature review, chapter 2) to calculate GRO and TWD.

Based on the methodology of Salomón et al. (2022), GRO values were processed afterwards by calculating the difference between the maximum and minimum for each tree and period. TWD values were divided in daily intervals, and maximum and minimum values of each day were averaged. Thus, one value of GRO and TWD per tree per period was worked out. After that, a ratio between dry and control period was calculated (i.e., GRO_{2018}/GRO_{2020}; $TWDmax_{2018}/TWDmax_{2020}$; $TWDmin_{2018}/TWDmin_{2020}$). Ratio values were decimals when control period obtained higher values than dry period, otherwise values reached numbers equals or higher to 1. We calculated the logarithm in base 10 for each ratio (log-transformed ratio hereafter).

The Stem Circadian Phases

For determining the stem circadian phases, the dendrometer data for each period was processed with the R package "dendrometeR"[4] (van der Maaten et al. 2016). As we described in the literature review (chapter 2), this package calculates the duration and magnitude (difference between maximum and minimum stem diameter value) of 3 circadian phases: 1) contraction, 2) expansion and 3) SRI. Also, a 4^{th} phase was calculated as a summary of all previous phases, which contained the duration and magnitude for the entire cycle. A log-transformed ratio was calculated for the maximum and mean values of mentioned circadian phases.

4.4.2. Meteorological and sap flow variables

Minimum and maximum values per day were calculated for VPD [KPa] and temperature [° C]. Hourly precipitation [mm] was cumulated by day and by month. To estimate stand transpiration, we upscaled sap flow [kg/h/tree] to the stand level. For upscaling, averaged tree sap flow values were divided by the mean cross-sectional area at 1.3 m height [m^2] and then was multiplied by basal area of the stand [m^2/ha].

[4] For more information about the package dendrometeR, see appendix 1.

Stand transpiration was compared with potential evapotranspiration, which was calculated by using penman-monteith equation (Zotarelli et al. 2015).

4.5. Statistical methods

4.5.1. T-test and Wilcoxon test

To determine if log-transformed ratios were significantly different from 0 we used a one tail T-test and Wilcoxon signed-rank test. For that, log-transformed ratios were classified into two groups: those which had normal distribution and those which not. The ones which fell in the first category were tested using a one tail T-test. The ones which fell in the second category were tested using Wilcoxon signed-rank test. To prove if they had normal distribution, we used a Shapiro test.

4.5.2. Generalized linear model for negative binomial distributions

The change in the duration of different circadian phases was predicted with generalised linear model (GLM) assuming a negative binomial distribution. We used magnitude [mm], phases of circadian cycle (contraction, expansion, and SRI), health status (attacked or healthy), and all possible combinations (Magnitude x Phases, Magnitude x Health status, Phases x Health status, Magnitude x Phases x Health status) as independent variables. Log-transformed duration was the dependent variable. A likelihood ratio was applied to determine which variables had a significant weight in the prediction of the duration.

The GLM was executed using the function glm.nb from the R package “MASS”. To apply this model, we used data from a sample of two healthy and attacked trees (n = 4). The model was calculated for three different periods, i) dry period (two years before the attack), ii) one month before the attack and iii) one month after the attack.

4.5.3. Correlations

GRO, TWD, the stem circadian phases and the stem size variation were correlated with meteorological and sap-flow data using the Spearman correlation. Also, we calculated the Spearman correlation between all approaches (GRO, TWD, stem circadian phases and stem size variation).

5. Results

5.1. The distribution of circadian phases during the year 2020

From a sample of 5 trees, tree code = 3A5, 3A8, 3C8, 3D3, 3D4; mean DBH = 34.8 cm, maximum DBH = 36 cm, minimum DBH = 33 cm (for more dimensions see table 2), we calculated the stem circadian phases from their automatic band dendrometers data using the R package dendrometeR (van der Maaten et al. 2016) (see Figure 13).We calculated the percentage of total hours of each phase for each month. Also, we calculated the total SRI per tree per month. The mean maximum and minimum values of all 5 studied trees were plotted with meteorological data (see Figure 14).

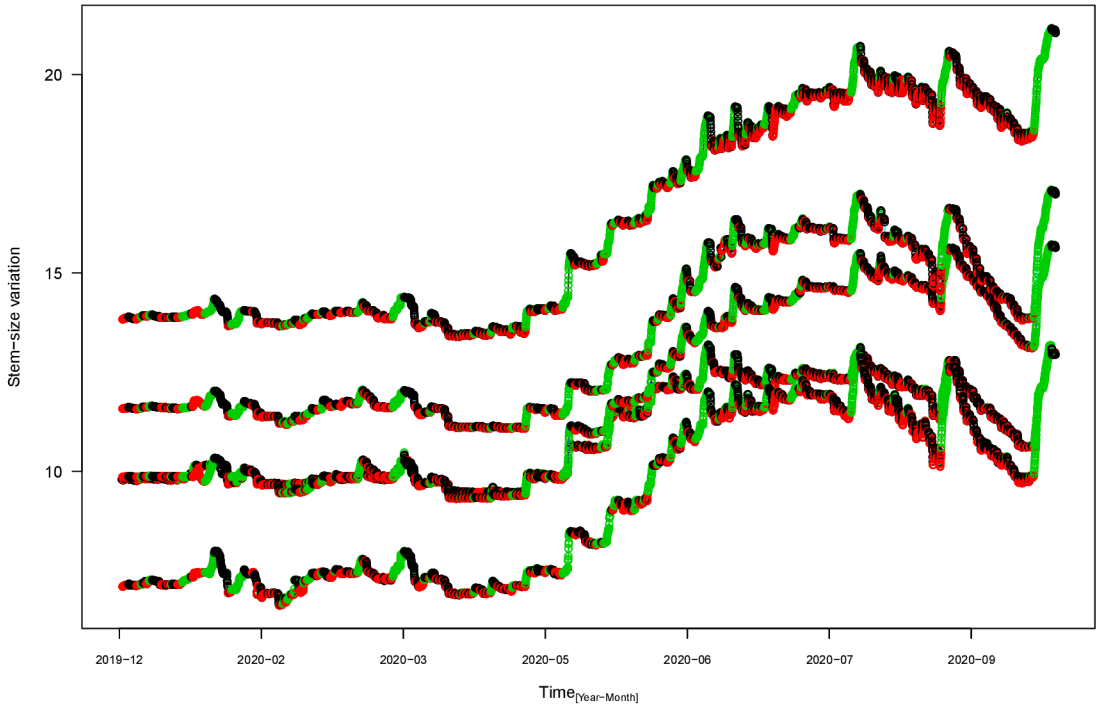

Figure 13: Circadian phases. Green colours represent the stem radius increment (SRI), red colour represent the expansion phase and black colour the contraction phase.

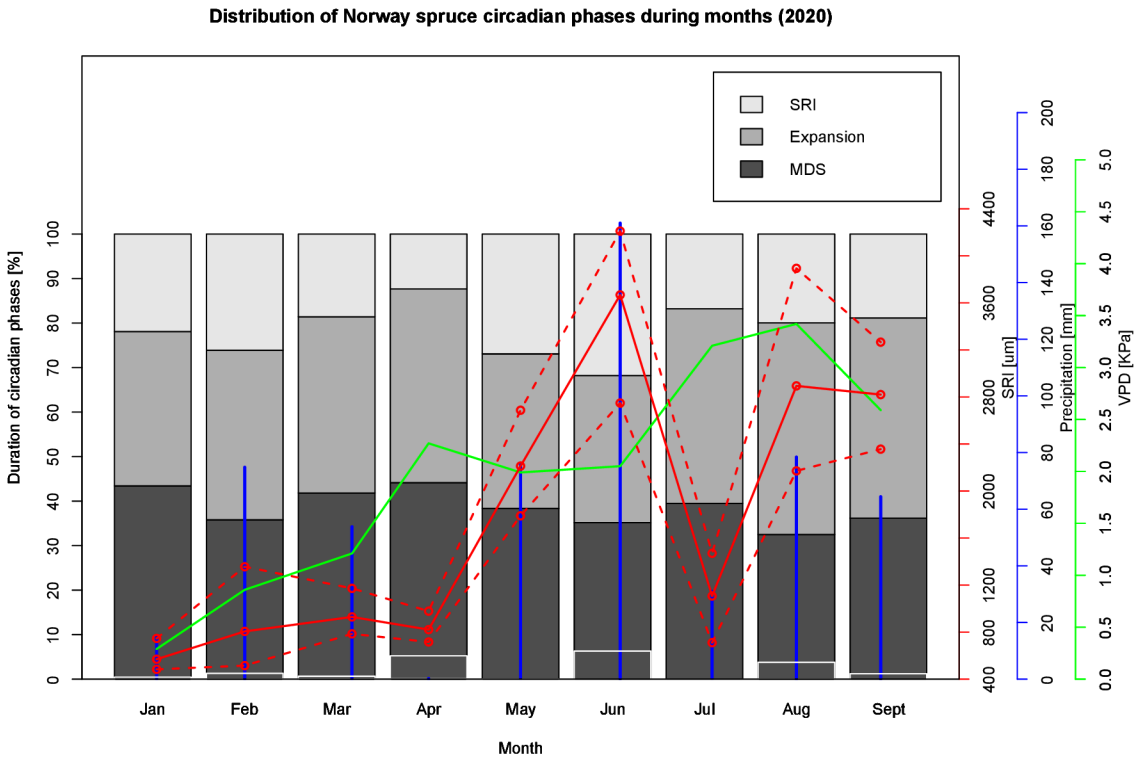

Figure 14: The duration [%] of the stem circadian phases per month during the year 2020. Red line shows the mean total SRI [µm] from 5 trees in each month. Dotted red lines shows the maximum and minimum SRI values. Green line shows the maximum values of vapor pressure deficit (VPD) [KPa] during the month. The blue bars are cumulated precipitation [mm] by month.

As it can be seen above, the SRI [µm] values reached their maximum when there was more quantity of precipitation (cumulated precipitation during June = 161.0 mm). The month of April had almost no precipitation (0.2 mm) and showed less variability between the maximum and minimum values of SRI [µm]. July showed decreasing SRI values with also a small amount of precipitation (31.0 mm) and high VPD values (3.21 KPa). Maximum values of VPD were reached in August (3.42 KPa).

The distribution of the phases in terms of duration was changing during the year. April was the month with the lowest percentage of SRI and also the month with the least rainfall (SRI = 12.33%, precipitation = 0.2 mm). This month had the highest percentage of MDS (44.13%). The month with the most SRI hours was June (31.8%), as the month with the most precipitation. The month with the lowest percentage of MDS was August (32.49%), which also had the highest percentage of expansion phase (47.54%).

5.2. The difference between dry and normal conditions

A daily approach was elaborated for a sample of 21 trees in control and dry periods. Positive values showed a correlation with precipitation, vapor pressure deficit and sap flow data (see Figure 15).

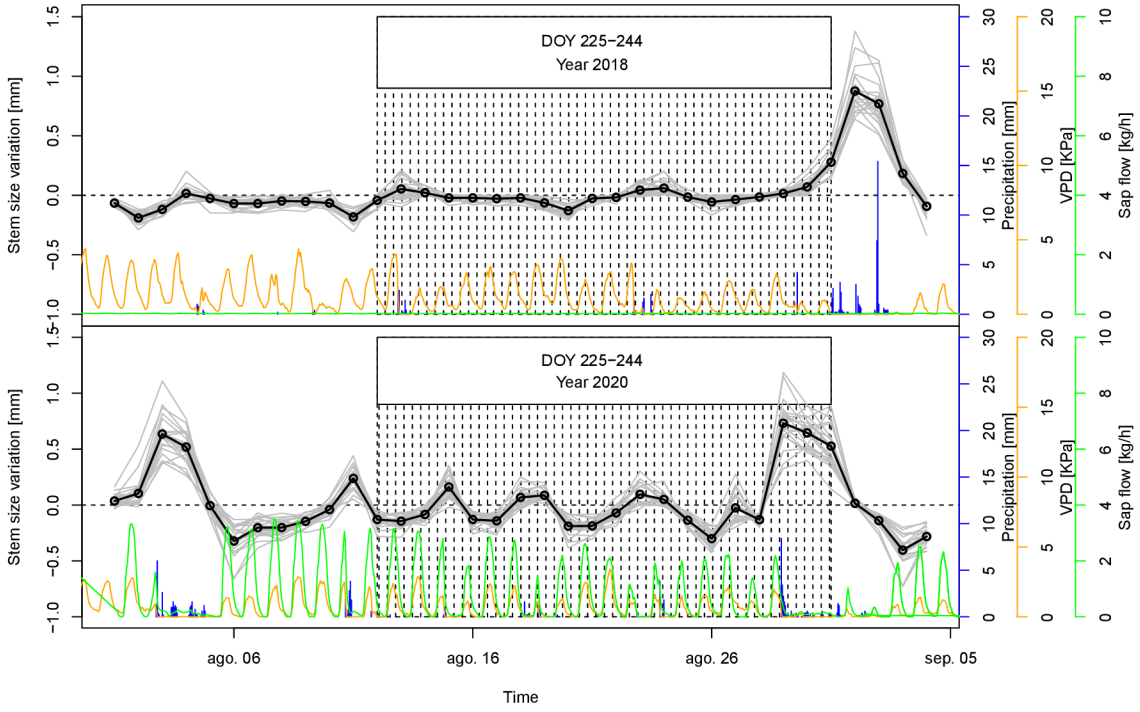

Figure 15: The daily approach for a sample of 21 trees. Grey lines show the stem size variation from individual trees [mm]. Black line is the average of individual values. Blue bars show precipitation in mm measured in hourly intervals. Orange line is vapor pressure deficit (VPD) [KPa] and green line the mean of the sap flow values of each tree [kg/h/tree]. Black dotted background shows the dry and control periods, 2018 and 2020 respectively.

As can be seen above, the humid year (2020) showed more variability in diameter fluctuations. Days with precipitation showed mostly positive values of stem radius variation. VPD values were higher on year 2018. Sap flow values were close to zero on year 2018. Due to the scale of the y axe in sap flow, the period from year 2018 had almost unrecognizable sap flow values. It is important to mention that the dry period was selected by looking into the soil water potential (see Figure 11), concretely for those values under the permanent wilting point, where trees cannot extract water from the soil. Thus, close to zero values in sap flow confirms that the tree water deficit was happening strongly in this stand.

Log-transformed ratios are shown in box plots (see Figure 16). Each box of the box plots contents the information that its inside the first and third quartile. Farther information is shown with bars and white points out of the boxes. The thicker black line represents the median. Crossed marks

shows where the average is. Negative log-transformed ratios are the result of lower values in the dry period (year 2018). Positive log-transformed ratios shows the opposite. Otherwise (Log-transformed ratio = 0), occurs when there is no difference between control and dry periods. Significant difference is calculated by t-test and Wilcoxon test *P-values* (Table 3).

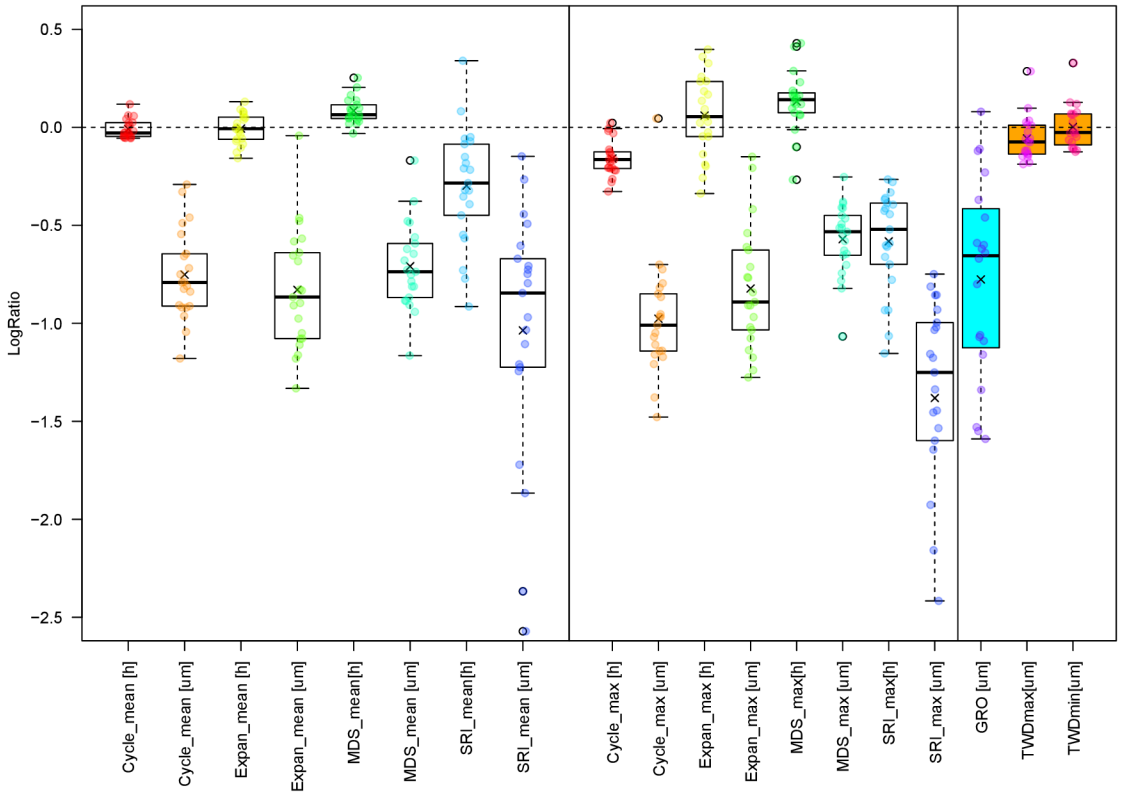

Figure 16: Log-transformed ratios for irreversible growth (GRO), minimum and maximum values of tree water deficit (TWD), and the mean and maximum values of duration [h] and magnitude [µm] of circadian phases in boxplots. Crosses and thicker black lines are mean and median values respectively. P-values *are shown in table 3.*

Log-transformed ratios showed a significant difference between the dry and control period for the maximum and mean values of magnitudes [µm] of all circadian phases. All these log-transformed ratios had negative values, showing that the dry period had lower values than the control period. GRO and maximum TWD were also significantly lower in the dry period. Log-transformed ratios calculated from duration [h], showed significantly lower values in the dry period in most of the circadian phases. Only the mean duration of contraction phase showed to be significantly longer in the dry period. The mean duration values of expansion phase, and the mean duration of the entire cycles had non-significant *p-values*. Minimum values of TWD did not show any significant difference from zero (see Table 3).

Table 3: Test and P*-values for the Log-transformed ratios*

	Units	Group Size	Shapiro test		Wilcoxon test		t-test		95% CI	
			W	P-value	V-statistic	P-value	t	P-value		
SRI mean	[h]	21	0.980	9.250E-01			-4.575	1.839E-04	-0.43; -0.16	***
MDS mean	[h]	21	0.945	2.780E-01			5.810	1.102E-05	0.05; 0.11	***
Expansion mean	[h]	21	0.980	9.230E-01			-0.361	7.221E-01	-0.04; 0.03	
Cycle mean	[h]	21	0.862	6.873E-03	83	2.722E-01			-0.04; 0.01	
SRI mean	[µm]	21	0.910	4.707E-02	0	9.537E-06			-1.30; -0.71	***
MDS mean	[µm]	21	0.974	8.272E-01			-7.443	3.489E-07	-1.33; -0.75	***
Expansion mean	[µm]	21	0.960	5.195E-01			-12.430	7.275E-11	-0.98; -0.69	***
Cycle mean	[µm]	21	0.964	6.002E-01			-15.051	2.261E-12	-0.86; -0.65	***
SRI max	[h]	21	0.905	4.436E-02	0	6.403E-05			-0.70; -0.43	***
MDS max	[h]	21	0.922	9.658E-02	206	8.516E-04			0.08; 0.19	***
Expansion max	[h]	21	0.975	8.328E-01			1.321	2.013E-01	-0.03; 0.16	
Cycle max	[h]	21	0.951	3.557E-01			-7.97	1.239E-07	-0.20; -0.12	***
SRI max	[µm]	21	0.903	4.036E-02	0	9.537E-07			-1.62; -1.10	***
MDS max	[µm]	21	0.954	4.116E-01			-11.82	1.77E-10	-1.63; -1.14	***
Expansion max	[µm]	21	0.954	3.992E-01			-12.01	1.341E-10	-0.97; -0.68	***
Cycle max	[µm]	21	0.863	7.248E-03	1	1.907E-06			-1.11; -0.89	***
GRO	[µm]	20	0.955	4.504E-01			-6.87	1.494E-06	-1.01; -0.54	***
TWD min	[µm]	20	0.886	2.301E-02	99	8.408E-01			-0.06; 0.05	
TWD max	[µm]	20	0.872	1.265E-02	42	1.718E-02			-0.12; -0.02	***

CI = Confidence intervals; SRI = Stem radius Increment; MDS = maximum daily shrinkage; GRO = irreversible growth; TWD = Tree Water Deficit; max = maximum values; min = minimum values

5.3. Healthy vs Attacked Trees

A daily approach was calculated for a sample of 4 trees (2 healthy and 2 attacked by the bark beetle) in three different periods: i) in the dry period of 2018, ii) one month before the attack of bark beetle, iii) after the attack of bark beetle. Trees showed a similar behaviour to meteorological variables by plotting the results of this approach (see Figure 17 and 18).

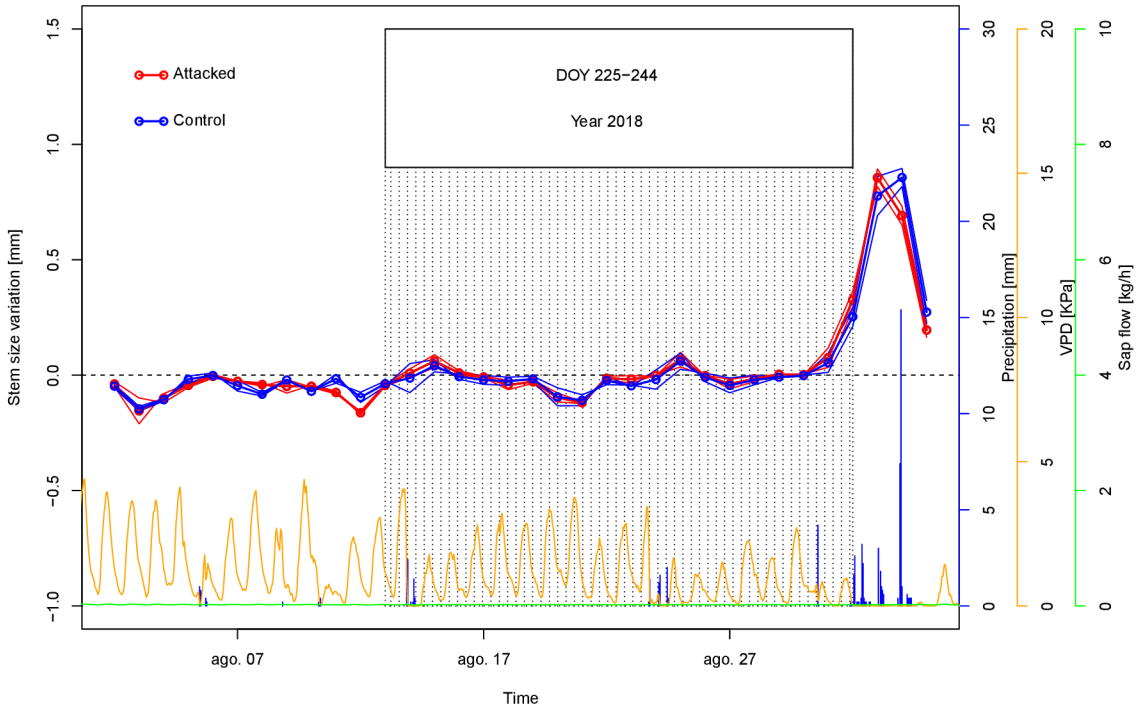

Figure 17: Daily approach of the dry period for healthy and attacked trees. Thin blue and red lines show the stem radius variation for control and attacked trees respectively. Thicker blue and red line are the average from control and attacked trees respectively. Blue bars are the precipitation [mm]. Orange line is the vapor pressure deficit VPD [KPa]. Green line is the mean of sap flow sensors [Kg/h/tree].

Stem radius variation for healthy and attacked trees showed small variability during the dry period. There was almost no difference in stem radius variation between healthy and attacked trees. Meteorological data from this plot is identical to the one shown in Figure 15 for the dry period. Sap flow values were close to zero.

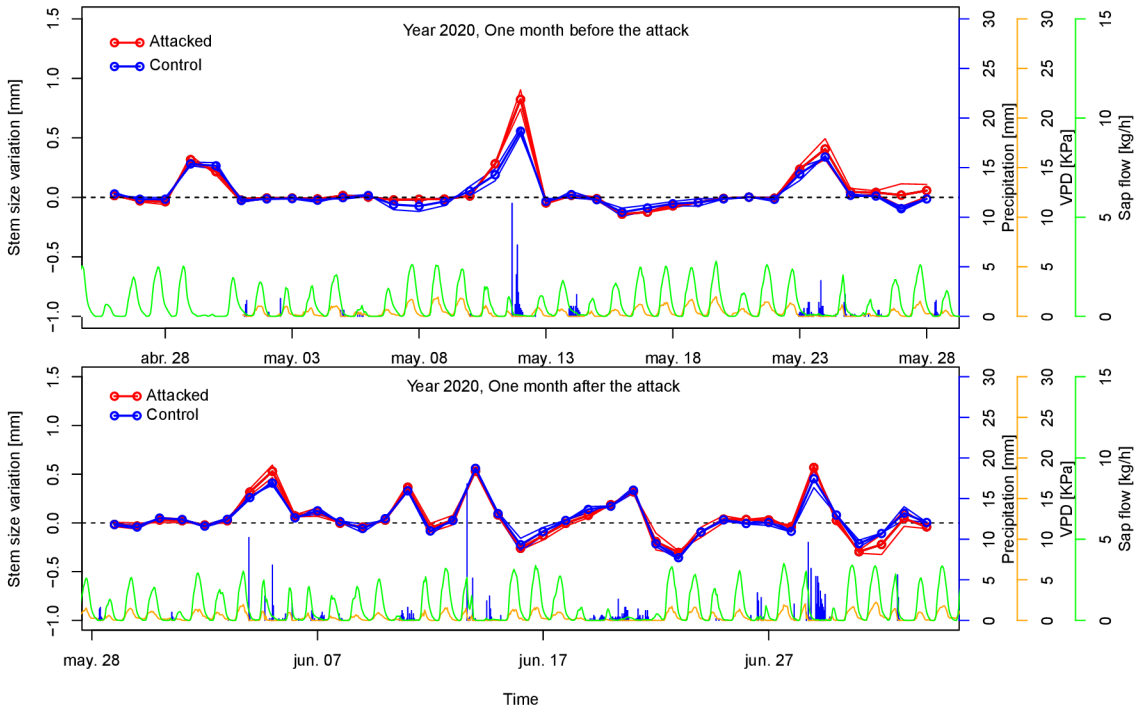

Figure 18: Daily approach of the dry period for healthy and attacked trees. Thin blue and red lines show the stem radius variation for control and attacked trees respectively. Thicker blue and red lines are the average of control and healthy trees respectively. Blue bars are the precipitation [mm]. Orange line is the vapor pressure deficit VPD [KPa]. Green line is the mean of sap flow sensors [Kg/h/tree].

As can be seen in the picture above, no difference between healthy and attacked trees can be detected with the daily approach. There were some gaps of meteorological data at the end of April.

A cycle approach for these trees and periods was calculated and analysed. Results from the cycle approach were fitted in a generalised linear model with a negative binomial distribution for each period. Diagnostic plots and detailed coefficients of all GLM can be found in Appendix 2. We estimated the effect of each predictor of our models using a likelihood ratio test (see Table 4,5 and 6).

Table 4: Likelihood-ratio test. Period = Dry (DOY 225-244, Year 2018)

Response: duration_m	Df	Deviance	Resid. Df	Resid. Dev	Pr(>Chi)	SC
			230	706,06		
magnitude	1	244,487	229	461,58	<2.2E-16	***
Health_status	1	0,078	228	461,5	7,80E-01	
phase	3	197,978	225	263,52	<2.2E-16	***
magnitude:Health_status	1	0,65	224	262,87	4,20E-01	
magnitude:phase	3	16,568	221	246,3	8,70E-04	***
Health_status:phase	3	6,157	218	240,14	1,04E-01	
magnitude:Health_status:phase	3	1,432	215	238,71	6,98E-01	
SC = Significant codes: '***' 0.001 '**' 0.01 '*' 0.05 '.' 0.1 ' ' 1						

Table 5: Likelihood-ratio test. Period = One month before the attack (DOY 117-147, Year 2020)

Response: duration_m	Df	Deviance	Resid. Df	Resid. Dev	Pr(>Chi)	SC
			285	836,95		
magnitude	1	224,451	284	612,5	<2E-16	***
Health_status	1	0,838	283	611,66	3,60E-01	
phase	3	226,417	280	385,25	<2E-16	***
magnitude:Health_status	1	6,552	279	378,69	1,05E-02	*
magnitude:phase	3	76,43	276	302,26	<2E-16	***
Health_status:phase	3	2,716	273	299,55	4,38E-01	
magnitude:Health_status:phase	3	2,405	270	297,14	4,93E-01	
SC = Significant codes: '***' 0.001 '**' 0.01 '*' 0.05 '.' 0.1 ' ' 1						

Table 6: Likelihood-ratio test. Period = One month after the attack (DOY 150-185, Year 2020)

Response: duration_m	Df	Deviance	Resid. Df	Resid. Dev	Pr(>Chi)	SC
			316	832,46		
magnitude	1	331,708	315	500,76	<2E-16	***
Health_status	1	2,996	314	497,76	8,35E-02	·
phase	3	141,376	311	356,38	<2E-16	***
magnitude:Health_status	1	0,035	310	356,35	8,51E-01	
magnitude:phase	3	19,525	307	336,82	2,13E-04	***
Health_status:phase	3	4,845	304	331,98	1,83E-01	
magnitude:Health_status:phase	3	3,154	301	328,82	3,69E-01	
SC = Significant codes: '***' 0.001 '**' 0.01 '*' 0.05 '.' 0.1 ' ' 1						

In the dry period of 2018, the predictable variable health status had no significant effect on the prediction of duration (X^2 = 0.078, p-value = n.s.). Also, any combination of predictable variables with health status had no significant effect on the prediction of the dependent variable. However, magnitude (X^2 = 244.487, p-value <2.2E-16), phases (X^2 = 197.978, p-value <2.2E-16) and its combinations (X^2 = 16.568, p-value = 8,70E-04) had

significant effect on the prediction of duration. The longer was the magnitude, the longer the duration. Contraction phase was the longest phase, followed by the expansion phase. SRI was the shortest phase.

The combination between health status and magnitude had a significant effect on the prediction of duration one month before the attack (X^2 = 6.552, p-value = 1.05E-02). Results from Wilcoxon rank test with continuity correction showed that there was not a significant difference between the magnitude of healthy and attacked trees (W = 10,424, p-value = 0.7315). Similar results were obtained by filtering the magnitude of SRI (W = 105, p-value = 0.5661). No statistical significance was found between the log-transformed duration of healthy and attacked trees (W = 10,615, p-value = 0.5371). Similar results were obtained by filtering the duration of SRI (W = 102, p-value = 0.4867).

The combination between health status and magnitude was no significant one month after the attack (X^2 = 0.035, p-value = n.s.). The single factor health status showed a significant effect in predicting the duration of the phases (X^2 = 2.996, p-value = 8,35E-02). Results from Wilcoxon rank test with continuity correction showed that there was not a significant difference between the magnitude of healthy and attacked trees after the attack of bark beetle (W = 12,186, p-value = 0.6462). Non-significant difference was found by filtering the magnitude of SRI (W = 246, p-value = 0.6925. No statistical significance was found between the log-transformed duration of healthy and attacked trees (W = 13,154, p-value = 0.4671). Similar results were obtained by filtering the duration of SRI (W = 1,878.5, p-value = 0.8339).

5.4. The Plant Water Status

The trees of site 3 showed higher values of transpiration in the control period than in the dry period (DOY 225-244, years 2020 and 2018). Hourly values in the dry period were close to 0 [mm/ha/h]. In the control period, values were close to 1 [mm/ha/h]. Potential evapotranspiration (Eo) was similar in both years, reaching daily total values around 6 [mm/ha/day]. Days with precipitation showed lower potential evapotranspiration (E_O = 0.5 [mm/ha/day]), and lower sap flow transpiration (E_Q = 0.08 [mm/ha/day]). Maximum daily E_Q was 0.97 [mm/ha/day], reached in the control period (DOY = 226). Maximum daily E_Q in the dry period was 0.001 [mm/ha/day] (DOY = 227) (see Figure 19 and table 7).

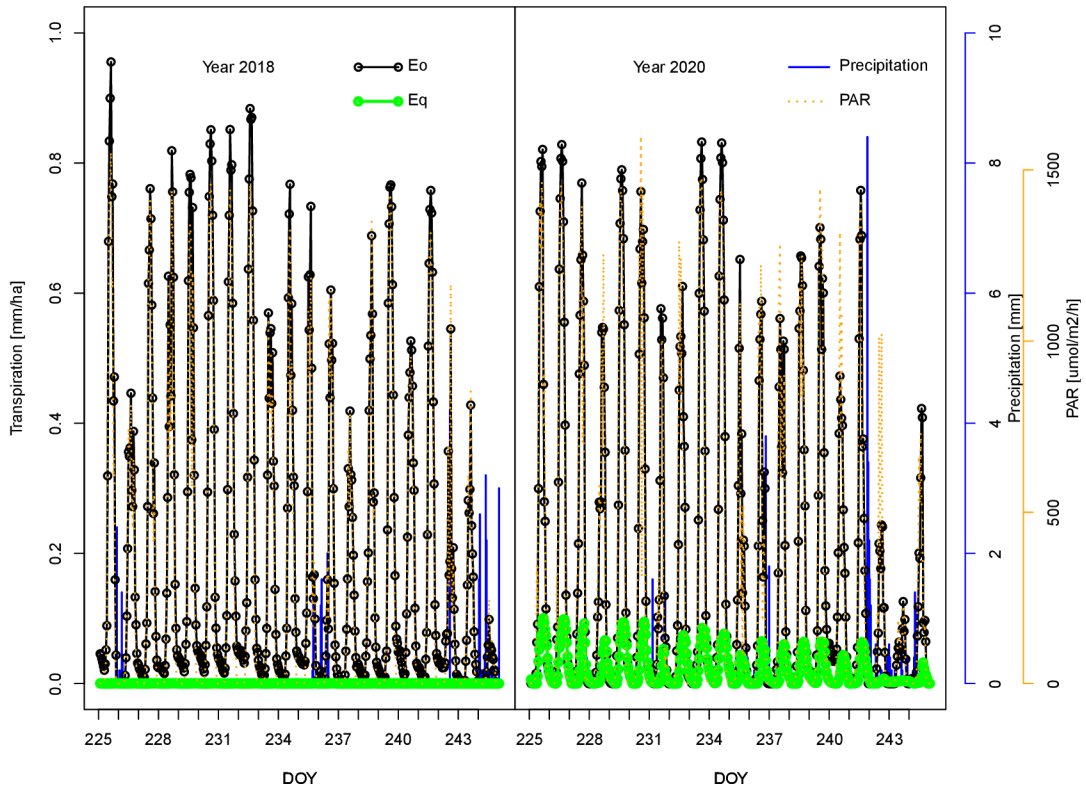

Figure 19: Hourly potential evapotranspiration (E_O) and stand transpiration (E_Q) in a dry period (year 2018) and a control period (year 2020) (DOY = 225-244). PAR = Photosynthetic Active Radiation [µmol/m²/h]. Blue bars are the daily precipitation [mm].

As it can be seen in the picture above, there are no difference of stand transpiration between day and night hours for the dry period. Even in days with precipitation trees did not response in terms of transpiration. However, in the humid period (year 2020), differences of stand transpiration can be observed between day and night hours. Also, trees of this period react to precipitation by decreasing or pausing transpiration. In the period of 2018, total stand transpiration was 0.018 mm/ha. While in the period of 2020 reached 10.692 mm/ha. Although, stand transpiration in 2020 was quite under the potential evapotranspiration.

Table 7: Daily stand transpiration and evapotranspiration in years 2020 and 2018

DOY	E_Q (2018) [mm/ha/day]	E_O (2018) [mm/ha/day]	E_Q (2020) [mm/ha/day]	E_O (2020) [mm/ha/day]
225	0,001	6,691	0,931	5,469
226	0,001	3,515	0,967	6,328
227	0,001	5,229	0,588	4,804
228	0,001	5,59	0,476	3,746
229	0,001	5,993	0,908	5,852
230	0,001	6,578	0,762	5,466
231	0,001	6,101	0,252	3,102
232	0,001	6,898	0,636	4,197
233	0,001	4,577	0,816	5,961
234	0,001	5,05	0,799	6,253
235	0,001	4,315	0,34	3,185
236	0,001	3,618	0,469	3,558
237	0,000	2,81	0,459	3,889
238	0,001	4,096	0,544	4,733
239	0,001	5,782	0,586	5,239
240	0,001	4,282	0,333	3,56
241	0,001	5,518	0,525	4,321
242	0,001	2,44	0,065	1,524
243	0,000	2,321	0,081	0,771
244	0,001	0,503	0,155	2,118

DOY = Day of the year; E_Q = Stand transpiration; E_O; Potential evapotranspiration

5.5. Correlations

Stem size variation was correlated using the Spearman correlation with different meteorological variables (see Figure 20). Maximum values per day were calculated for Temperature, VPD and sap flow. Precipitation was cumulated per day. Also, minimum temperature per day was calculated. Stem radius variation was split into positive and negative values.

*Figure 20: Spearman Correlation between stem radius variation (amplitude) and meteorological variables (included sap flow). MaxT = maximum temperature. MinT = minimum temperature. Prec = Precipitation. MaxVPD = maximum vapor pressure deficit. Max. Sap = maximum sap flow. Significant codes: '***' 0.001 '**' 0.01 '*' 0.05 '.' 0.1 ' ' 1*

All meteorological variables were correlated with the stem radius variation (amplitude) except minimum temperature. Correlation between precipitation and positive values of stem radius variation was significant (rho = 0.651, *p-value* = 3.047e-06). Maximum VPD and sap flow were correlated with stem radius variation (rho = -0.538, *p-value* = 2.958e-04 and rho = -0.417, *p-value* = 6.423e-03, respectively). However, only maximum VPD was correlated with negative values of stem radius variation (rho = -0.398, *p-value* = 1.26e-02). No other variables were correlated with negative values of stem radius variation (Precipitation rho =0.069, Maximum temperature rho = -0.216, Maximum sap flow rho = -0.311, *p-values* =n.s.). Minimum temperatures were not correlated with stem radius variation (rho = -0.030 for negative stem radius variation and 0.208 for positive stem radius variation; *P-value* = n.s.).

Duration [h] and magnitude [mm] from the stem circadian phases (1 = contraction, 2 = expansion, 3 = SRI and 4 = entire cycle) were correlated using the Spearman correlation with different meteorological variables (see Figure 21). A correlation between magnitude

and duration was also calculated. Maximum values per cycle were calculated for Temperature, VPD and sap flow using the R-package dendrometeR. Precipitation was cumulated per cycle.

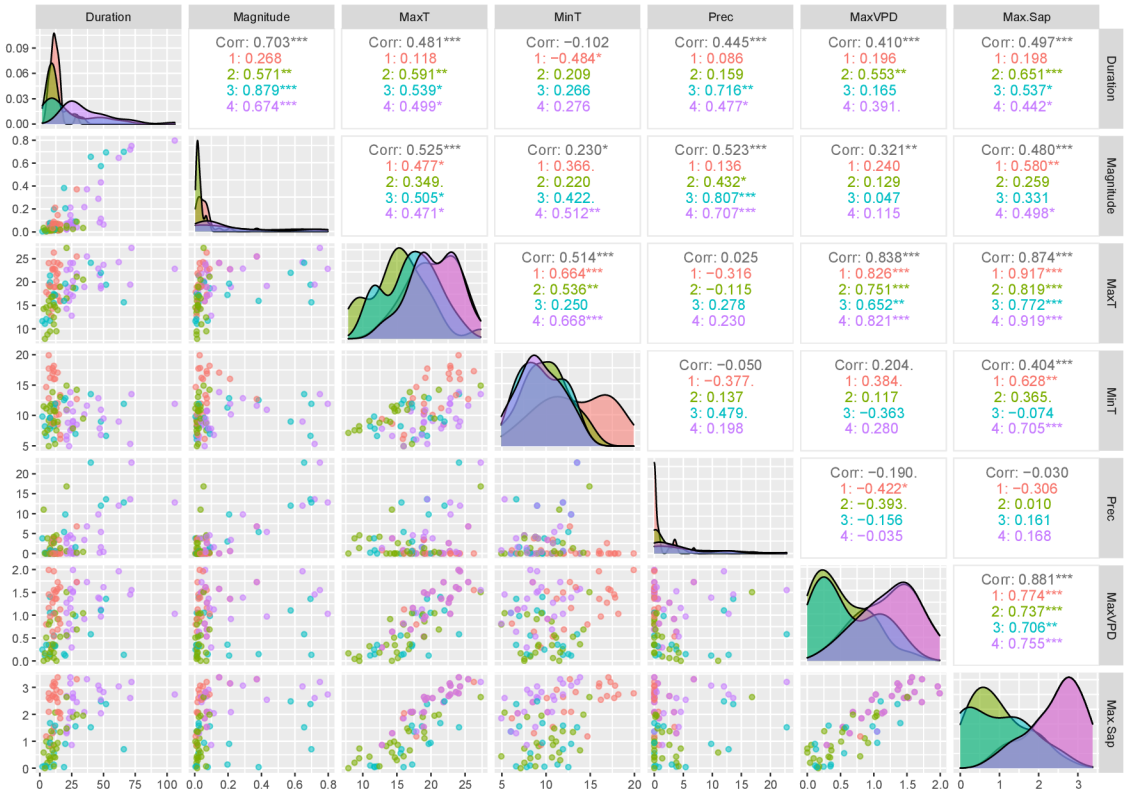

*Figure 21: Spearman Correlation between different phases of circadian cycle and meteorological data (included sap flow). Phase 1 = contraction. Phase 2 = expansion. Phase 3 = SRI. Phase 4 = complete cycle. MaxT = maximum temperature. MinT = minimum temperature. Prec = Precipitation. MaxVPD = maximum vapor pressure deficit. Max. Sap = maximum sap flow. Significant codes: '***' 0.001 '**' 0.01 '*' 0.05 '.' 0.1 ' ' 1*

In terms of duration, maximum temperatures were correlated with phases 2, 3 and 4 (rho = 0.591; 0.539; 0.499, *p-values* = 2.380e-03; 2.544e-02; 1.116e-02). Phase 1 was not correlated with this meteorological variable (rho = 0.118, *p-value* = n.s.). Only phase 1 was correlated with minimum temperatures (rho = -0.484, *p-value* = 1.428e-02). Rest of the phases were not correlated with minimum temperatures (rho = 0.209; 0.266 and 0.276 for phases 2,3,4 respectively. *p-values* = n.s.). Phases 3 and 4 were correlated with precipitation (rho = 0.716; 0.477, *p-values* = 1.234e-03; 1.582e-02), but not phases 1 and 2 (rho = 0.086; 0.159, *p-values* = n.s.). Phases 2 and 4 were correlated with maximum values of VPD (rho = 0.553; 0.391, *p-values* = 5.019e-03; 5.325e-02). Phases 1 and 3 were not correlated with VPD (rho = 0.196; 0.65, *p-values* = n.s.). Maximum sap flow

values were correlated with phases 2, 3 and 4 (rho = 0.651; 0.537; 0.442, *p-values* = 5.690e-04; 2.625e-02; 2.710e-02) but not with phase 1 (rho = 0.198, *p-value* = n.s.).

As for the magnitude, all phases were correlated with maximum temperature (rho = 0.477; 0.349; 0.505; 0.471, *p-values* = 1.581e-02; 9.545e-02; 4.079e-02; 1.858e-02). Minimum temperatures were correlated with phases 1 and 4 (rho = 0.366; 0.512, *p-values* = 7.178e-02; 9.683e-03), but not with phases 2 and 3 (rho = 0.220; 0.422, *p-values* = n.s.). Precipitation was correlated with phases 2, 3 and 4 significantly (rho = 0.432; 0.807; 0.707, *p-values* = 3.504e-02; 9.191e-05; 7.715e-05), but not with phase 1 (rho = 0.136; *p-value* = n.s.). Maximum VPD was correlated with the magnitude of all combined phases (rho =0.321; *p-value* = 1.907e-03), but not with any filtered phase of the cycle (rho = 0.240; 0.129; 0.047; 0.115, *p-values* = n.s.). Maximum sap-flow was correlated with phase 1 and 4 (rho = 0.580; 0.498, *p-values* = 2.387e-03; 1.213e-02). However, it was not correlated with phases 2 and 3 (*p-values* = 0.259; 0.331)

Magnitude and duration of phases 2, 3 and 4 were significantly correlated between them (rho = 0.571; 0.879; 0.674, *p-value*s = 3.571e-03; 3.331e-06; 2.182e-04). However, magnitude and duration were not correlated for phase 1 (rho = 0.268, *p-value*s = 1.95e-01). Correlation between different phases of the cycle approach, maximum and minimum values of daily approach, GRO and maximum and minimum values of TWD were correlated between them (see Figure 22).

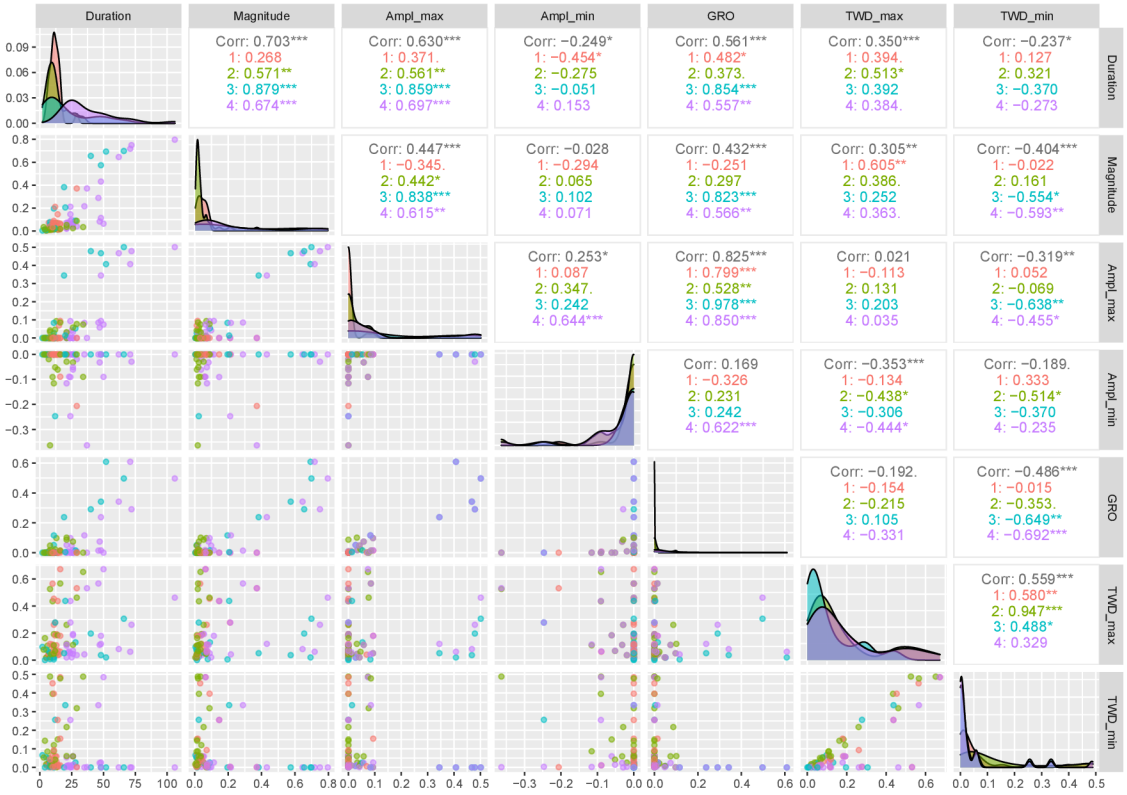

*Figure 22: Spearman Correlation between different phases of circadian cycle with other approaches. Phase 1 = contraction. Phase 2 = expansion. Phase 3 = SRI. Phase 4 = complete cycle. Ampl_max = positive stem size variation. Ampl_min = negative stem size variation. TWD_max = maximum tree water deficit. TWD_min = minimum tree water deficit. Significant codes: '***' 0.001 '**' 0.01 '*' 0.05 '.' 0.1 ' ' 1.*

Different phases of circadian phases were correlated with other approaches. All magnitude and duration phases were correlated with the maximum values of stem radius variation (highest correlation with phase 3, rho = 0.838 and *p-value* = 2.623e-05 for magnitude, and rho = 0.859 and *p-value* = 9.819e-06 for duration). However, for the minimum values of stem radius variation, only phase 1 of duration was correlated (rho = -0.454, *p-value* = 2.279e-02). All phases of duration were correlated with irreversible growth (GRO) (highest correlation with phase 3, rho = 0.854, *p-value* = 1.269e-05). GRO was only correlated with phases 3 and 4 of magnitude (rho = 0.823; 0.566, *p-values* = 4.976e-05; 3.219e-03). Maximum values of TWD were correlated with phases 1, 2 and 4, for both duration and magnitude variables (highest correlation for phase 1 of magnitude rho = 0.605, *p-value* = 1.352e-03). However, it was not correlated with phase 3, neither for magnitude and duration (rho = 0.392; 0.252, *p-values* = n.s.). Minimum values of TWD only were correlated with phases 3 and 4 of magnitude (rho = -0.554; -0.593, *p-values* = 2.113e-02; 1.770e-03).

6. Discussion

6.1. The distribution of SRI during year 2020

Our SRI results confirmed that the trees were physiologically active during the months of January to March. However, these months showed a small amount of SRI values compared to other months of the year. From March to June, SRI values increased continuously. In July, SRI values dropped sharply. In August, SRI values increased again and remained constant until September. These results are similar to the observations of (Vieira et al. 2013), who studied the seasonal cycle, in maritime pine (*Pinus pinaster* Ait.) on the west coast of Portugal. These authors named the period from January to March as the "winter dormancy" and the continuous increase in stem radius from March to June as the "spring rehydration".

The highest SRI values were reached in June. June was also the month with more proportion of SRI in terms of duration. These results went hand by hand with (King et al. 2013), who observed that the maximum values and variation of SRI were detected in June in larch and spruce species in the central Swiss Alps. However, these authors did not identify a true spring rehydration period.

The month with the highest proportion of SRI hours was June, being the month with the most precipitation. April was the month with the lowest proportion of SRI hours and also the month with the least precipitation. The correlation between SRI duration and precipitation strengthens this theory. We suggest that the monthly proportions of SRI hours are highly dependent on the amount of precipitation.

6.2. The drought effect on the stem circadian cycle

Our results supported one of the hypotheses established by Salomón et al. (2022), which considered the 2018 heat wave as a limitation of the GRO. We observed a significant reduction in GRO in the dry period that covered the same time period as the heatwave. In addition, SRI values, which were highly correlated with GRO, were also significantly lower in the dry period.

On the other hand, our results showed that the maximum TWD values were significantly higher in the wet period and the minimum TWD values were not significantly different between the dry and normal periods. Contrary to the findings of Salomon et al. (2022), which showed significantly higher TWD values in the dry period. However, these authors

were studying 21 tree species with automatic dendrometers. One of these tree species, namely *Picea sitchensis*, showed lower TWD values in the dry period as we did.

Our results showed that the duration of the contraction phase was significantly longer in the dry period. Nevertheless, the magnitudes of contractions were significantly reduced in the dry period, which is in line withresults of (Balducci et al. 2019) who observed a significant increase in shrinkage duration in black spruce (*Picea mariana* (Mill.)) under controlled conditions of water deficit and heat in a greenhouse in Chicoutimi, Canada. They also confirmed that the magnitude of this phase was significantly reduced.

We observed that the expansion phase was significantly shorter in the dry period in terms of magnitude. The duration of the expansion phase was not significantly different between the dry and control periods. A similar conclusion was reached by Balducci et al. (2019) in terms of magnitude. However, contrary to their findings, we did not obtain the same results in terms of duration, where they observed a significantly shorter duration of the expansion phase in the dry period. The reason that could explain this difference is that they divided the circadian phases into contraction and expansion, thus including the SRI in the expansion phase. Vieira et al. (2013) also noted the fact that the climate response of duration was less clear than that of magnitude.

Cycle results (phase 4) were in accordance with the results of the individual phases. Mean values of the magnitude of phase 4 were significantly lower in the dry period, due to the fact that all individual phases were lower for this period. In terms of duration, the mean values of the entire cycles were not significantly different between the dry and the control periods. All maximum values for the entire cycle were significantly lower in the dry period.

6.3. The bark beetle effect on the circadian cycle

Our results showed no significant differences in the magnitude and duration of the different circadian phases between healthy and attacked trees. However, likelihood ratios showed that the categorical parameter "health status" was a significant variable in predicting the duration of circadian phases one month before and after the bark beetle attack. Thus, our results suggest that the duration of phases could be a key factor in understanding bark beetle preference for tree selection. These results are in line with Wullschleger, McLaughlin and Ayres (2004), who observed in a loblolly pine (*Pirzus taeda* L.) forest that the slowest tree, in terms of growth, was notably infested by the pine

beetle (*Dendroctonus frorztalis* Zirnm.). After the bark bettle attack, the variation in stem circumference was small. These authors also observed that the two fastest growing trees were among the last to be attacked by pine beetles. Since bark beetle attacks have been observed also on healthy (fast-growing) trees, differences in phase duration between healthy and attacked trees cannot be considered a prerequisite for successful beetle attack, but probably a preference. However, due to our small sample of trees and localities, it is dangerous to generalise from these results.

Our observations showed non-significant difference between healthy and attacked trees during the dry period. They all reacted independently to drought stress. However, we had a small sample of trees to study (2 healthy and 2 attacked), and the attack was far from the dry period (dry period in 2018, attack occurred in 2020). We propose to study more trees with automatic dendrometers that have been attacked by bark beetle during a dry period or a few months after the dry period. We recommend selecting dry periods as we have done in this thesis. Measurements of soil water potential and sap flow can show that the water demand of the trees has not been supplied.

6.4. Plant water status

Our observations suggest that during the dry period the trees had no water available in the soil. Trees were almost unable to transpire water from the soil. Observations from the European Alps showed that trees reduce their transpiration rates slowly with decreasing availability of soil water resources, and only show large reductions in water use after specific thresholds are exceeded (Anfodillo et al. 1998; Clausnitzer et al. 2011). One reason to explain why transpiration in our stand did not decrease slowly could be that the dry period already started earlier than we expected. We selected dry periods by looking at the soil water potential, namely when the soil water potential reached values below -15 bar. Probably, dry conditions for our trees started with higher soil water potential values. (Krejza et al. 2021) also suggested that Norway spruce trees are more sensitive to drought because Norway spruce roots do not reach great depths, especially at altitudinal levels of 600 m a.s.l.

The control period (year 2020 with wet conditions) had constant levels of transpiration with good weather conditions. Stand transpiration reacted to weather variables by decreasing or pausing sap flow during rainy or cloudy days. This fact has been broadly

observed by other authors, especially in *Pinus sylvestris* (L.) and *Picea abies* (L.) Karst. (Cienciala et al. 1998; Köstner et al. 1996; Schulze et al. 1985).

6.5. Correlations between circadian phases and meteorological variables

Similar to our observations, a significant negative correlation between shrinkage phase magnitude and maximum temperature was also observed by (Vieira et al. 2013) in autumn in maritime pine. Vieira et al. (2013) pointed out that this observation was related to low soil water content. When soil water content is low, stomatal control over transpiration rates becomes stronger. This stronger control of transpiration has a negative effect on stem contraction, reducing it.

Our observations showed a significant correlation between the magnitude of the contraction phase and sap flow. However, the correlation between the duration of the contraction phase and sap flow was not significant. Similar to us, (Deslauriers, Rossi, Anfodillo 2007) observed a significant correlation between the magnitude of the contraction phase and sap flow. These authors also observed a significant correlation between the duration of contraction phase and sap flow. However, their study was carried out over a longer period of time (1996-2004) and in a mixed forest (*Larix decidua* Mill., *Pinus cembra* L. and *Picea abies* L. Karst.) at 2080 m.a.s.l. near the Cinque Torri mountain (northeastern Italian Alps).

Our results also found a significant correlation in the magnitude and duration of SRI with precipitation. The magnitude of the expansion phase with precipitation was also significantly correlated. The duration of the expansion phase was not significantly correlated with precipitation. The magnitude and duration of the contraction phase were not significantly correlated with precipitation. Similar to our observations, (Deslauriers, Rossi, Anfodillo 2007) found a non-significant correlation between the duration and magnitude of the contraction phase and precipitation. As for expansion, these authors observed a positive and significant correlation with precipitation (for both duration and magnitude). However, these authors did not divide the circadian phases as we did. They included the SRI in the expansion phase.

Our results showed that the correlations between the magnitude of circadian phases and VPD were not significant. The duration of the contraction phase and the duration of phase 4 were significantly correlated with the maximum VPD values. Similar observations were found by (Liu et al. 2017), who studied the intra-annual variation of stem radius of *Larix*

principis-rupprechtii in the Liupan Mountains of northwest China. They divided tree growth into three stages. In the second stage, they found significant correlations between contraction phase and VPD. In the third stage, the correlation between the magnitude of circadian phases and VPD was not significant.

6.6. Other correlations

We observed a negative correlation between the maximum values of stem radius variation and VPD. (Fan 2016) showed similar results in an Asian tropical dry karst forest.

Our results were similar to those of Deslauriers, Rossi, Anfodillo (2007) by correlating the stem size variation (daily approach) with the magnitude of the cycle approach. We observed a Spearman correlation coefficient of 0.62 between the maximum values of the daily approach and the phase 4 of the circadian cycle. The correlation had a significant *P-value*. These authors showed a Pearson correlation coefficient between 0.84 and 0.61 depending on the year, also with a significant *P-value*.

Our results showed that there is no significant correlation between stem size variation, calculated with the daily approach, and the duration of circadian cycles. (Biondi, Rossi 2015) observed a positive correlation between these two variables. However, they transformed duration and stem size variation using the logarithm.

Our observations support the fact that during positive TWD values, trees are not growing (Zweifel et al. 2016). Maximum values of TWD were significantly correlated with the duration of phases 1 (contraction), 2 (expansion) and 4 (full cycle). The correlation between these variables were also significant in terms of magnitude. The highest correlation was found between the magnitude of the contraction phase and the maximum values of TWD. Duration of phase 3 (SRI) was not significantly correlated with TWD. The magnitude of phase 3 was also not significantly correlated with maximum values of TWD. Minimum values of TWD were negatively correlated with the magnitude of SRI.

Our results showed that all phases of duration were significantly correlated with GRO, being the highest correlation with SRI. The magnitude of SRI and the phase 4 were also significantly correlated with GRO. To our knowledge, correlations between GRO and SRI obtained with the package dendrometeR (van der Maaten et al. 2016), have not been done yet. We consider the correlations between these variables to be consistent because they both quantify tree growth.

7. Conclusion

Our description of the circadian phases during the year 2020 showed that Norway spruce trees were physiologically active during the months of January to March. Months with the least rainfall showed the smallest amount of SRI. The month of June showed the highest SRI values, being also the month with more precipitation. The duration of circadian phases kept almost constant during the months. The months from October to December were not evaluated due to a lack of automatic dendrometer data.

In terms of magnitude, significant difference was found between the dry and normal periods for all maximum and mean values of different circadian phases. The dry period had significant lower values than the control period. GRO and maximum TWD were also significantly lower in the dry period. The duration of contraction phase was significantly lower in the dry period. The mean duration of expansion phase did not show significant difference between dry and control periods. Minimum values of TWD did not show significant difference between dry and control periods.

The binomial factor "health status" (attacked or healthy trees) was a significant independent variable to predict the duration of phases between healthy and attacked trees one month after the attack of bark beetle. The combination between the independent variables "health status" and "magnitude of phases" was a significant factor to predict the duration of circadian phases one month before the attack. During dry conditions (two years before the attack), "health status" and any of its combinations with other variables was not significant to predict the duration of phases between healthy and attacked trees. Neither the duration nor the variation in stem size was significantly different between control and attacked trees.

The evaluation of plant water status showed that during the dry period trees were not able to transpire water from soil. Soil water potential confirmed that soil was under the permanent wilting point, strengthening the fact that trees could not reach water from soil. Trees were able to transpire during the control period.

Precipitation proved to be the strongest meteorological variable influencing SRI. Sap flow was significantly correlated with contraction phase. Temperature and VPD were correlated with different phases of circadian cycle, showing similar results that were published before by other authors.

8. References

ANFODILLO, Tommaso, RENTO, Stefano, CARRARO, Vinicio, FURLANETTO, Luca, URBINATI, Carlo and CARRER, Marco, 1998. Tree water relations and climatic variations at the alpine timberline: seasonal changes of sap flux and xylem water potential in Larix decidua Miller, Picea abies (L.) Karst. and Pinus cembra L. *Annales des Sciences Forestières*. Online. 1998. Vol. 55, no. 1–2, pp. 159–172. [Accessed 25 March 2022]. DOI 10.1051/forest:19980110.

AUGUSTO, Laurent, RANGER, Jacques, BINKLEY, Dan and ROTHE, Andreas, 2002. Impact of several common tree species of European temperate forests on soil fertility. *Annals of Forest Science*. Online. 1 April 2002. Vol. 59, no. 3, pp. 233–253. [Accessed 19 February 2022]. DOI 10.1051/forest:2002020.

BAIER, Peter, PENNERSTORFER, Josef and SCHOPF, Axel, 2007. PHENIPS—A comprehensive phenology model of Ips typographus (L.) (Col., Scolytinae) as a tool for hazard rating of bark beetle infestation. *Forest Ecology and Management*. Online. 30 September 2007. Vol. 249, no. 3, pp. 171–186. [Accessed 20 February 2022]. DOI 10.1016/j.foreco.2007.05.020.

BALDUCCI, Lorena, DESLAURIERS, Annie, ROSSI, Sergio and GIOVANNELLI, Alessio, 2019. Stem cycle analyses help decipher the nonlinear response of trees to concurrent warming and drought. *Annals of Forest Science*. Online. September 2019. Vol. 76, no. 3, pp. 1–18. [Accessed 26 March 2022]. DOI 10.1007/s13595-019-0870-7.

BARRIOPEDRO, David, FISCHER, Erich M., LUTERBACHER, Jürg, TRIGO, Ricardo M. and GARCÍA-HERRERA, Ricardo, 2011. The Hot Summer of 2010: Redrawing the Temperature Record Map of Europe. *Science*. Online. 8 April 2011. Vol. 332, no. 6026, pp. 220–224. [Accessed 24 February 2022]. DOI 10.1126/science.1201224.

BELIEN, Evelyn, ROSSI, Sergio, MORIN, Hubert and DESLAURIERS, Annie, 2014. High-resolution analysis of stem radius variations in black spruce [Picea mariana (Mill.) BSP] subjected to rain exclusion for three summers. *Trees*. 1 October 2014. Vol. 28, pp. 1257–1265. DOI 10.1007/s00468-014-1011-4.

BIONDI, Franco and ROSSI, Sergio, 2015. Plant-water relationships in the Great Basin Desert of North America derived from Pinus monophylla hourly dendrometer records. *International Journal of Biometeorology*. Online. 1 August 2015. Vol. 59, no. 8, pp. 939–953. [Accessed 26 March 2022]. DOI 10.1007/s00484-014-0907-4.

BRÁZDIL, R., TRNKA, M., DOBROVOLNÝ, P., CHROMÁ, K., HLAVINKA, P. and ŽALUD, Z., 2009. Variability of droughts in the Czech Republic, 1881–2006. *Theoretical and Applied Climatology*. Online. 1 August 2009. Vol. 97, no. 3, pp. 297–315. [Accessed 3 April 2022]. DOI 10.1007/s00704-008-0065-x.

BRINKMANN, Nadine, EUGSTER, Werner, ZWEIFEL, Roman, BUCHMANN, Nina and KAHMEN, Ansgar, 2016. Temperate tree species show identical response in tree water deficit but different sensitivities in sap flow to summer soil drying. *Tree Physiology*. Online. 1 December 2016. Vol. 36, no. 12, pp. 1508–1519. [Accessed 24 February 2022]. DOI 10.1093/treephys/tpw062.

BURCKLE, L. and GRISSINO-MAYER, H. D., 2003. Stradivari, violins, tree rings, and the Maunder Minimum: a hypothesis. *Dendrochronologia*. Online. 1 January 2003. Vol. 21, no. 1, pp. 41–45. [Accessed 19 February 2022]. DOI 10.1078/1125-7865-00033.

CAMPBELL, Gaylon S. and NORMAN, John M., 1998. Water Vapor and Other Gases. In: CAMPBELL, Gaylon S. and NORMAN, John M. (eds.), *An Introduction to Environmental Biophysics*. Online. New York, NY: Springer. pp. 37–51. [Accessed 25 March 2022]. ISBN 978-1-4612-1626-1.

CAUDULLO, Giovanni, WELK, Erik and SAN-MIGUEL-AYANZ, Jesús, 2017. Chorological maps for the main European woody species. *Data in Brief*. Online. 1 June 2017. Vol. 12, pp. 662–666. [Accessed 5 March 2022]. DOI 10.1016/j.dib.2017.05.007.

CAVEY, Joe, PASSOA, Steven and KUCERA, Dan, 1994. *Screening Aids for Exotic Bark Beetles in the Northeastern United States*. United States Department of Agriculture, Forest Service, Northeastern Area.

CIENCIALA, Emil, KUCERA, Jiri, RYAN, Michael G. and LINDROTH, Anders, 1998. Water flux in boreal forest during two hydrologically contrasting years; species specific regulation of canopy conductance and transpiration. *Annales des Sciences Forestières*. Online. 1998. Vol. 55, no. 1–2, pp. 47–61. [Accessed 2 March 2022]. DOI 10.1051/forest:19980104.

CLAUSNITZER, Falko, KÖSTNER, Barbara, SCHWÄRZEL, Kai and BERNHOFER, Christian, 2011. Relationships between canopy transpiration, atmospheric conditions and soil water availability—Analyses of long-term sap-flow measurements in an old Norway spruce forest at the Ore Mountains/Germany. *Agricultural and Forest Meteorology*. 1 August 2011. Vol. 151, pp. 1023–1034. DOI 10.1016/j.agrformet.2011.04.007.

DESLAURIERS, Annie, MORIN, Hubert, URBINATI, Carlo and CARRER, Marco, 2003. Daily weather response of balsam fir (Abies balsamea (L.) Mill.) stem radius increment from dendrometer analysis in the boreal forests of Québec (Canada). *Trees*. Online. 1 November 2003. Vol. 17, no. 6, pp. 477–484. [Accessed 25 February 2022]. DOI 10.1007/s00468-003-0260-4.

DESLAURIERS, Annie, ROSSI, Sergio and ANFODILLO, Tommaso, 2007. Dendrometer and intra-annual tree growth: What kind of information can be inferred? *Dendrochronologia*. Online. 6 September 2007. Vol. 25, no. 2, pp. 113–124. [Accessed 24 February 2022]. DOI 10.1016/j.dendro.2007.05.003.

DESLAURIERS, Annie, ROSSI, Sergio, TURCOTTE, Audrey, MORIN, Hubert and KRAUSE, Cornélia, 2011. A three-step procedure in SAS to analyze the time series from automatic dendrometers. *Dendrochronologia*. Online. 1 January 2011. Vol. 29, no. 3, pp. 151–161. [Accessed 25 February 2022]. DOI 10.1016/j.dendro.2011.01.008.

DREW, David M. and DOWNES, Geoffrey M., 2009. The use of precision dendrometers in research on daily stem size and wood property variation: A review. *Dendrochronologia*. Online. 1 January 2009. Vol. 27, no. 2, pp. 159–172. [Accessed 25 February 2022]. DOI 10.1016/j.dendro.2009.06.008.

FAN, Ze-Xin, 2016. Stem radial growth in response to microclimate in an Asian tropical dry karst forest. *Acta Ecologica Sinica*. 10 October 2016. Vol. 36, pp. 401–409. DOI 10.1016/j.chnaes.2016.09.005.

GARG, Ankit, BORDOLOI, Sanandam, GANESAN, Suriya Prakash, SEKHARAN, Sreedeep and SAHOO, Lingaraj, 2020. A relook into plant wilting: observational evidence based on unsaturated soil–plant-photosynthesis interaction. *Scientific Reports*. Online. 16 December 2020. Vol. 10, no. 1, pp. 22064. [Accessed 5 March 2022]. DOI 10.1038/s41598-020-78893-z.

HAHN, Daniel A. and DENLINGER, David L., 2007. Meeting the energetic demands of insect diapause: Nutrient storage and utilization. *Journal of Insect Physiology*. Online. 1 August 2007. Vol. 53, no. 8, pp. 760–773. [Accessed 21 February 2022]. DOI 10.1016/j.jinsphys.2007.03.018.

HANEWINKEL, Marc, CULLMANN, Dominik A., SCHELHAAS, Mart-Jan, NABUURS, Gert-Jan and ZIMMERMANN, Niklaus E., 2013. Climate change may cause severe loss in the economic value of European forest land. *Nature Climate Change*. Online. March 2013. Vol. 3, no. 3, pp. 203–207. [Accessed 1 April 2022]. DOI 10.1038/nclimate1687.

HOLUŠA, Jaroslav, LUBOJACKÝ, Jan, ČURN, Vladislav, TONKA, Tomáš, LUKÁŠOVÁ, Karolina and HORÁK, Jakub, 2018. Combined effects of drought stress and Armillaria infection on tree mortality in Norway spruce plantations. *Forest Ecology and Management*. Online. 1 November 2018. Vol. 427, pp. 434–445. [Accessed 19 February 2022]. DOI 10.1016/j.foreco.2018.01.031.

HULCR, Jiri, ATKINSON, Thomas H., COGNATO, Anthony I., JORDAL, Bjarte H. and MCKENNA, Duane D., 2015. Chapter 2 - Morphology, Taxonomy, and Phylogenetics of Bark Beetles. In: VEGA, Fernando E. and HOFSTETTER, Richard W. (eds.), *Bark Beetles*. Online. San Diego: Academic Press. pp. 41–84. [Accessed 21 February 2022]. ISBN 978-0-12-417156-5.

Ips typographus (L.), European Spruce Bark Beetle Screening Aid, no date. Online. [Accessed 21 February 2022]. Retrieved from: https://www.barkbeetles.org/exotic/htypgrph.html

KING, Gregory, FONTI, Patrick, NIEVERGELT, Daniel, BÜNTGEN, Ulf and FRANK, David, 2013. Climatic drivers of hourly to yearly tree radius variations along a 6°C natural warming gradient. *Agricultural and Forest Meteorology*. Online. 15 January 2013. Vol. 168, pp. 36–46. [Accessed 25 March 2022]. DOI 10.1016/j.agrformet.2012.08.002.

KIRKHAM, M. B., 2005. 8 - Field Capacity, Wilting Point, Available Water, and the Non-Limiting Water Range. In: KIRKHAM, M. B. (ed.), *Principles of Soil and Plant Water Relations*. Online. Burlington: Academic Press. pp. 101–115. [Accessed 5 March 2022]. ISBN 978-0-12-409751-3.

KÖSTNER, B., BIRON, P., SIEGWOLF, R. and GRANIER, A., 1996. Estimates of water vapor flux and canopy conductance of Scots pine at the tree level utilizing different xylem sap flow methods. *Theoretical and Applied Climatology*. Online. 1 March 1996. Vol. 53, no. 1, pp. 105–113. [Accessed 27 March 2022]. DOI 10.1007/BF00866415.

KREJZA, Jan, CIENCIALA, Emil, SVETLIK, Jan, BELLAN, Michal, ESTELLE, Noyer, HORACEK, Petr, STEPANEK, Petr and MAREK, Michal, 2021. Evidence of climate-induced stress of Norway spruce along elevation gradient preceding the current dieback in Central Europe. *Trees*. 1 February 2021. Vol. 35. DOI 10.1007/s00468-020-02022-6.

LIDÓN, A., RAMOS, C. and RODRIGO, A., 1999. Comparison of drainage estimation methods in irrigated citrus orchards. *Irrigation Science*. Online. 1 November 1999. Vol. 19, no. 1, pp. 25–36. [Accessed 5 March 2022]. DOI 10.1007/s002710050068.

LIU, Zebin, WANG, Yanhui, TIAN, Ao, YU, Pengtao, XIONG, Wei, XU, Lihong and WANG, Yarui, 2017. Intra-Annual Variation of Stem Radius of Larix principis-rupprechtii and Its Response to Environmental Factors in Liupan Mountains of Northwest China. *Forests*. Online. October 2017. Vol. 8, no. 10, pp. 382. [Accessed 29 March 2022]. DOI 10.3390/f8100382.

LOBINGER, G., 1994. Air temperature as a limiting factor for flight activity of two species of pine bark beetles, Ips typographus L. and Pityogenes chalcographus L. (Col., Scolytidae). *Anzeiger fuer Schaedlingskunde, Pflanzenschutz, Umweltschutz (Germany)*. Online. 1994. [Accessed 21 February 2022]. Retrieved from: https://scholar.google.com/scholar_lookup?title=Air+temperature+as+a+limiting+factor+for+flight+activity+of+two+species+of+pine+bark+beetles%2C+Ips+typographus+L.+and+Pityogenes+chalcographus+L.+%28Col.%2C+Scolytidae%29&author=Lobinger%2C+G.+%28Landesanstalt+fuer+Wald+und+Forstwirtschaft%2C+Freising+%28Germany%29%29&publication_year=1994

MAREK, Michal V., JANOUŠ, Dalibor, TAUFAROVÁ, Klára, HAVRÁNKOVÁ, Kateřina, PAVELKA, Marian, KAPLAN, Věroslav and MARKOVÁ, Irena, 2011. Carbon exchange between ecosystems and atmosphere in the Czech Republic is affected by climate factors. *Environmental Pollution*. Online. 1 May 2011. Vol. 159, no. 5, pp. 1035–1039. [Accessed 1 April 2022]. DOI 10.1016/j.envpol.2010.11.025.

MATTHEWS, Bradley, NETHERER, Sigrid, KATZENSTEINER, Klaus, PENNERSTORFER, Josef, BLACKWELL, Emma, HENSCHKE, Patrick, HIETZ, Peter, ROSNER, Sabine, JANSSON, Per-Erik, SCHUME, Helmut and SCHOPF, Axel, 2018. Transpiration deficits increase host susceptibility to bark beetle attack: Experimental observations and practical outcomes for Ips typographus hazard assessment. *Agricultural and forest meteorology*. Online. 2018. [Accessed 30 March 2022]. Retrieved from: https://dx.doi.org/10.1016/j.agrformet.2018.08.004

MCMANUS, Michael L. and LIEBHOLD, Andrew M., 2003. *Proceedings--ecology, Survey, and Management of Forest Insects: Kraków, Poland, September 1-5, 2002*. USDA Forest Service, Northeastern Research Station. Google-Books-ID: 5bZIib8Kn6wC

MISHRA, Ashok K. and SINGH, Vijay P., 2010. A review of drought concepts. *Journal of Hydrology*. Online. 14 September 2010. Vol. 391, no. 1, pp. 202–216. [Accessed 26 February 2022]. DOI 10.1016/j.jhydrol.2010.07.012.

NETHERER, Sigrid, KANDASAMY, Dineshkumar, JIROSOVÁ, Anna, KALINOVÁ, Blanka, SCHEBECK, Martin and SCHLYTER, Fredrik, 2021. Interactions among Norway spruce, the bark beetle Ips typographus and its fungal symbionts in times of drought. *Journal of Pest Science*. Online. 1 June 2021. Vol. 94, no. 3, pp. 591–614. [Accessed 27 March 2022]. DOI 10.1007/s10340-021-01341-y.

PRACIAK, Andrew, DIXON, Christopher, FYSON, George E., RUSHFORTH, Keith, SASSEN, Marieke, SHEIL, Douglas, CORREIA, Cristina Sousa, TEELING, Claire and VAN HEIS, Miriam, 2013. *The CABI Encyclopedia of Forest Trees*. CABI. ISBN 978-1-78064-236-9. Google-Books-ID: cBf4AgAAQBAJ

RAHMSTORF, Stefan and COUMOU, Dim, 2011. Increase of extreme events in a warming world. *Proceedings of the National Academy of Sciences*. Online. 1 November 2011. Vol. 108, no. 44, pp. 17905–17909. [Accessed 21 February 2022]. DOI 10.1073/pnas.1101766108.

RAI, Raveendra Kumar, SINGH, Vijay P. and UPADHYAY, Alka, 2017. Chapter 17 - Soil Analysis. In: RAI, Raveendra Kumar, SINGH, Vijay P. and UPADHYAY, Alka (eds.), *Planning and Evaluation of Irrigation Projects*. Online. Academic Press. pp. 505–523. [Accessed 5 March 2022]. ISBN 978-0-12-811748-4.

ROLTSCH, William J., ZALOM, Frank G., STRAWN, Ann J., STRAND, Joyce F. and PITCAIRN, Michael J., 1999. Evaluation of several degree-day estimation methods in California climates. *International Journal of Biometeorology*. Online. 1 March 1999. Vol. 42, no. 4, pp. 169–176. [Accessed 21 February 2022]. DOI 10.1007/s004840050101.

SALLÉ, A., KERDELHUÉ, C., BRETON, M. and LIEUTIER, F., 2003. Characterization of microsatellite loci in the spruce bark beetle Ips typographus (Coleoptera: Scolytinae). *Molecular Ecology Notes*. Online. 2003. Vol. 3, no. 3, pp. 336–337. [Accessed 21 February 2022]. DOI 10.1046/j.1471-8286.2003.00443.x.

SALOMÓN, Roberto L., PETERS, Richard L., ZWEIFEL, Roman, SASS-KLAASSEN, Ute G. W., STEGEHUIS, Annemiek I., SMILJANIC, Marko, POYATOS, Rafael, BABST, Flurin, CIENCIALA, Emil, FONTI, Patrick, LERINK, Bas J. W., LINDNER, Marcus, MARTINEZ-VILALTA, Jordi, MENCUCCINI, Maurizio, NABUURS, Gert-Jan, VAN DER MAATEN, Ernst, VON ARX, Georg, BÄR, Andreas, AKHMETZYANOV, Linar, BALANZATEGUI, Daniel, BELLAN, Michal, BENDIX, Jörg, BERVEILLER, Daniel, BLAŽENEC, Miroslav, ČADA, Vojtěch, CARRARO, Vinicio, CECCHINI, Sébastien, CHAN, Tommy, CONEDERA, Marco, DELPIERRE, Nicolas, DELZON, Sylvain, DITMAROVÁ, Ľubica, DOLEZAL, Jiri, DUFRÊNE, Eric, EDVARDSSON, Johannes, EHEKIRCHER, Stefan, FORNER, Alicia, FROUZ, Jan, GANTHALER, Andrea, GRYC, Vladimír, GÜNEY, Aylin, HEINRICH, Ingo, HENTSCHEL, Rainer, JANDA, Pavel, JEŽÍK, Marek, KAHLE, Hans-Peter, KNÜSEL, Simon, KREJZA, Jan, KUBERSKI, Łukasz, KUČERA, Jiří, LEBOURGEOIS, François, MIKOLÁŠ, Martin, MATULA, Radim, MAYR, Stefan, OBERHUBER, Walter, OBOJES, Nikolaus, OSBORNE, Bruce, PALJAKKA, Teemu, PLICHTA, Roman, RABBEL, Inken, RATHGEBER, Cyrille B. K., SALMON, Yann, SAUNDERS, Matthew, SCHARNWEBER, Tobias, SITKOVÁ, Zuzana, STANGLER, Dominik Florian, STEREŃCZAK, Krzysztof, STOJANOVIĆ, Marko, STŘELCOVÁ, Katarína, SVĚTLÍK, Jan, SVOBODA, Miroslav, TOBIN, Brian, TROTSIUK, Volodymyr,

URBAN, Josef, VALLADARES, Fernando, VAVRČÍK, Hanuš, VEJPUSTKOVÁ, Monika, WALTHERT, Lorenz, WILMKING, Martin, ZIN, Ewa, ZOU, Junliang and STEPPE, Kathy, 2022. The 2018 European heatwave led to stem dehydration but not to consistent growth reductions in forests. *Nature Communications*. Online. 10 January 2022. Vol. 13, no. 1, pp. 28. [Accessed 18 February 2022]. DOI 10.1038/s41467-021-27579-9.

SAN-MIGUEL-AYANZ, J., DE RIGO, Daniele, CAUDULLO, Giovanni, DURRANT, Tracy, MAURI, Achille, TINNER, Willy, BALLIAN, Dalibor, BECK, Pieter, BIRKS, Harry, EATON, Edward, ENESCU, Cristian, SALVATORE, Pasta, POPESCU, Ioana, RAVAZZI, Cesare, WELK, Erik, ABAD VIÑAS, Raul, AZEVEDO, João, BARBATI, Anna, BARREDO, José and ZECCHIN, Barbara, 2016. *European Atlas of Forest Tree Species*. ISBN 978-92-79-36740-3.

SCHULZE, E. -D., ČERMÁK, J., MATYSSEK, M., PENKA, M., ZIMMERMANN, R., VASÍCEK, F., GRIES, W. and KUČERA, J., 1985. Canopy transpiration and water fluxes in the xylem of the trunk of Larix and Picea trees — a comparison of xylem flow, porometer and cuvette measurements. *Oecologia*. Online. 1 July 1985. Vol. 66, no. 4, pp. 475–483. [Accessed 27 March 2022]. DOI 10.1007/BF00379337.

SMITH, D.M. and ALLEN, S.J., 1996. Measurement of sap flow in plant stems. *Journal of Experimental Botany*. Online. 1 December 1996. Vol. 47, no. 12, pp. 1833–1844. [Accessed 5 March 2022]. DOI 10.1093/jxb/47.12.1833.

STOEL, Berend C. and BORMAN, Terry M., 2008. A Comparison of Wood Density between Classical Cremonese and Modern Violins. *PLOS ONE*. Online. 2 July 2008. Vol. 3, no. 7, pp. e2554. [Accessed 19 February 2022]. DOI 10.1371/journal.pone.0002554.

STÖHR, Andreas and LÖSCH, Rainer, 2004. Xylem sap flow and drought stress of Fraxinus excelsior saplings. *Tree Physiology*. Online. 1 February 2004. Vol. 24, no. 2, pp. 169–180. [Accessed 24 February 2022]. DOI 10.1093/treephys/24.2.169.

SURMIŃSKI, Janusz, 2007. Wood Properties and Uses. In: TJOELKER, Mark G., BORATYŃSKI, Adam and BUGAŁA, Władysław (eds.), *Biology and Ecology of Norway Spruce*. Online. Dordrecht: Springer Netherlands. pp. 333–342. [Accessed 30 March 2022]. ISBN 978-1-4020-4841-8.

SVENNING, Jens-Christian and SKOV, Flemming, 2004. Limited filling of the potential range in European tree species. *Ecology Letters*. Online. 2004. Vol. 7, no. 7, pp. 565–573. [Accessed 19 February 2022]. DOI 10.1111/j.1461-0248.2004.00614.x.

TARIQ, Akash, PAN, Kaiwen, OLATUNJI, Olusanya Abiodun, GRACIANO, Corina, LI, Zilong, SUN, Feng, ZHANG, Lin, WU, Xiaogang, CHEN, Wenkai, SONG, Dagang, HUANG, Dan, XUE, Tan and ZHANG, Aiping, 2018. Phosphorous fertilization alleviates drought effects on Alnus cremastogyne by regulating its antioxidant and osmotic potential. *Scientific Reports*. Online. 4 April 2018. Vol. 8, no. 1, pp. 5644. [Accessed 30 March 2022]. DOI 10.1038/s41598-018-24038-2.

TAYLOR, R. J., MORIN, Nancy R. and PRESS, Oxford University, 1993. *Flora of North America: Volume 2: Pteridophytes and Gymnosperms*. Committee. ISBN 978-0-19-508242-5.

TESKEY, Robert, WERTIN, Timothy, BAUWERAERTS, Ingvar, AMEYE, Maarten, MCGUIRE, Mary Anne and STEPPE, Kathy, 2015. Responses of tree species to heat waves and extreme heat events. *Plant, Cell & Environment*. Online. 2015. Vol. 38, no. 9, pp. 1699–1712. [Accessed 24 February 2022]. DOI 10.1111/pce.12417.

VAN CAMP, Janne, HUBEAU, Michiel, VAN DEN BULCKE, Jan, VAN ACKER, Joris and STEPPE, Kathy, 2018. Cambial pinning relates wood anatomy to ecophysiology in the African tropical tree Maesopsis eminii. *Tree Physiology*. Online. 1 February 2018. Vol. 38, no. 2, pp. 232–242. [Accessed 24 February 2022]. DOI 10.1093/treephys/tpx151.

VAN DER MAATEN, Ernst, 2013. Thinning prolongs growth duration of European beech (Fagus sylvatica L.) across a valley in southwestern Germany. *Forest Ecology and Management*. Online. 15 October 2013. Vol. 306, pp. 135–141. [Accessed 16 March 2022]. DOI 10.1016/j.foreco.2013.06.030.

VAN DER MAATEN, Ernst, VAN DER MAATEN-THEUNISSEN, Marieke, SMILJANIĆ, Marko, ROSSI, Sergio, SIMARD, Sonia, WILMKING, Martin, DESLAURIERS, Annie, FONTI, Patrick, VON ARX, Georg and BOURIAUD, Olivier, 2016. dendrometeR: Analyzing the pulse of trees in R. *Dendrochronologia*. Online. 1 December 2016. Vol. 40, pp. 12–16. [Accessed 24 February 2022]. DOI 10.1016/j.dendro.2016.06.001.

VIEIRA, Joana, ROSSI, Sergio, CAMPELO, Filipe, FREITAS, Helena and NABAIS, Cristina, 2013. Seasonal and daily cycles of stem radial variation of Pinus pinaster in a drought-prone environment. *Agricultural and Forest Meteorology*. 1 October 2013. Vol. 180, pp. 173–181. DOI 10.1016/j.agrformet.2013.06.009.

WERMELINGER, B. and SEIFERT, M., 1998. Analysis of the temperature dependent development of the spruce bark beetle Ips typographus (L) (Col., Scolytidae). *Journal of Applied Entomology*. Online. 1998. Vol. 122, no. 1–5, pp. 185–191. [Accessed 21 February 2022]. DOI 10.1111/j.1439-0418.1998.tb01482.x.

WULLSCHLEGER, Stan, MCLAUGHLIN, Samuel and AYRES, Matthew, 2004. High-resolution analysis of stem increment and sap flow for loblolly pine trees attacked by southern pine beetle. *Canadian Journal of Forest Research-revue Canadienne De Recherche Forestiere - CAN J FOREST RES*. 1 November 2004. Vol. 34, pp. 2387–2393. DOI 10.1139/x04-118.

ZOTARELLI, L., DUKES, M., ROMERO, C., MIGLIACCIO, K. and KELLY, T., 2015. Step by Step Calculation of the Penman-Monteith Evapotranspiration (FAO-56 Method) 1. *undefined*. Online. 2015. [Accessed 31 March 2022]. Retrieved from: https://www.semanticscholar.org/paper/Step-by-Step-Calculation-of-the-Penman-Monteith-1-Zotarelli-Dukes/8c7a164802368a05710ade7acc0f38d9b136f8be

Zpráva o stavu lesa a lesního hospodářství 2020 (Lesy, eAGRI), 2021. Online. [Accessed 5 March 2022]. Retrieved from:

https://eagri.cz/public/web/mze/lesy/lesnictvi/zprava-o-stavu-lesa-a-lesniho/zprava-o-stavu-lesa-a-lesniho-2020.html

ZSCHEISCHLER, Jakob, WESTRA, Seth, VAN DEN HURK, Bart J. J. M., SENEVIRATNE, Sonia I., WARD, Philip J., PITMAN, Andy, AGHAKOUCHAK, Amir, BRESCH, David N., LEONARD, Michael, WAHL, Thomas and ZHANG, Xuebin, 2018. Future climate risk from compound events. *Nature Climate Change*. Online. June 2018. Vol. 8, no. 6, pp. 469–477. [Accessed 24 February 2022]. DOI 10.1038/s41558-018-0156-3.

ZWEIFEL, Roman, HAENI, Matthias, BUCHMANN, Nina and EUGSTER, Werner, 2016. Are trees able to grow in periods of stem shrinkage? *New Phytologist*. Online. 2016. Vol. 211, no. 3, pp. 839–849. [Accessed 24 February 2022]. DOI 10.1111/nph.13995.